NGU
Geology for Society since 1858

Skagerrak Aeromagnetic Survey 1996
SAS-96

GEUS

HYDRO

Mobil

PHILLIPS 66

STATOIL

Report 97.022

SAS-96 Part II
Skagerrak Aeromagnetic Survey 1996
Interpretation Report

NGU
Norges geologiske undersøkelse
Geological Survey of Norway

Geological Survey of Norway
P.O.Box 3006 - Lade
N-7002 Trondheim, Norway
Tel.: 47 73 90 40 11
Telefax 47 73 92 16 20

REPORT

Report no.: 97.022 | ISSN 0800-3416 | Grading: ÅPEN

Title:
SAS-96 Part II, Skagerrak Aeromagnetic Survey 1996, Interpretation Report

Authors:
Odleiv Olesen, Mark Smethurst, Les Beard, Trond Torsvik, NGU, Torben Bidstrup, GEUS and Bernt Egeland, NPD

Clients:
GEUS, Mobil Exploration, Norsk Hydro, NPD, Phillips Petroleum, Statoil and NGU

County:

Commune:

Map-sheet name (M=1:250.000)
Arendal, Mandal and Uddevalla

Map-sheet no. and -name (M=1:50.000)

Deposit name and grid-reference:

Number of pages: 56 Price (NOK): Kr. 298,-
Map enclosures: 7

Fieldwork carried out:	Date of report:	Project no.:	Person responsible:
April-June 1996	13.05.1997	2698.00	Jan S. Rønning

Summary:
Potential field data in the Norwegian-Danish Basin have been interpreted. The aeromagnetic anomaly pattern is found to represent three types of magnetic sources: 1) deep magnetic basement. 2) Permian volcanics and intrusives, and 3) buried sand channels of Quaternary age. The positive gravity effect from the shallow Moho below the Norwegian-Danish Basin is not sufficient to compensate for the highly reduced gravity effect from the light sediments within the basin. More dense material has to be introduced at depth in the crust below the basin. We have chosen to add a body of mafic rock immediately above the Moho. It is thickest (10 km) below the deepest part of the westermost Norwegian-Danish Basin and get thinner towards the east. The basement depth of the bulk of the Norwegian-Danish Basin varies between 6 and 8 km. Depths between 3 km and 9 km were obtained along the Farsund Basin, and the magnetic anomaly pattern indicates a complex system of fault blocks along the Sorgenfrei-Tornquist Zone. Circular gravity anomalies in the Norwegian-Danish Basin most likely represent mafic intrusive or extrusive complexes of Precambrian (Sveconorwegian), late Palaeozoic or Mesozoic age. Since they are located on a row along the mid-axis of the basin they may be related to the thinning of the crust. These isolated intrusions could represent the initial phase of the formation of an axial dyke along the deepest part of the basin. Some of the aeromagnetic anomalies within the Norwegian-Danish Basin may be attributed to magnetic basement. The negative aeromagnetic anomaly in the Farsund Basin is more likely related to the Proterozoic Rogaland Igneous Complex than to Permian or Tertiary volcanism which has earlier been suggested. The aeromagnetic data indicate that the belt of magnetic Proterozoic granites along the Mandal-Ustaoset Fault Zone continues below the Farsund Basin where it seems to be dextrally offset by approximately 10 km along the Sorgenfrei-Tornquist Zone. This constitutes the accumulated offset during several deformation periods from late Proterozoic to Cenozoic time. A very distinct set of high frequency NE-SW to ENE-WSW trending anomalies occurring regionally in the southeastern part of the SAS-96 area are caused by shallow Pleistocene sand channels (typically of 200-300 m thickness and 2000 m width buried below 100 m of younger sediments). These sand channels seem to occur widely beneath the northern continental shelf and lowlands of Europe. They are the erosive analogues of eskers in areas of soft, deformable bedrock. The aeromagnetic method has proved to be an adequate tool for mapping sand channels in the North Sea.

Keywords: Geofysikk	Kontinentalsokkel	Tolkning
Berggrunnsgeologi	Magnetometri	
Petrofysikk	Gravimetri	Fagrapport

CONTENTS

1 INTRODUCTION

The objective of the Skagerrak Aeromagnetic Survey 1996 (SAS-96) was to acquire new aeromagnetic data in the Skagerrak and the southeastern North Sea and to interpret the geology of this area in light of new and existing potential field data. The project is a collaboration between the Geological Survey of Denmark and Greenland (GEUS), Mobil Exploration Norway, Norsk Hydro, the Norwegian Petroleum Directorate (NPD), Phillips Petroleum, Statoil and the Geological Survey of Norway (NGU).

The southeastern North Sea and Skagerrak area has been studied by several workers. Most studies have concentrated on seismic data, although a few (Sharma 1970, Sellevoll & Aalstad 1971, Åm 1973, Hospers & Rathore 1984, Sindre 1993) have included aeromagnetic data. The Geological Survey of Norway (NGU) conducted an aeromagnetic survey offshore Denmark, Norway and Sweden from c. 56° 15'N to c. 58°N (Fig. 3.1) during April to June 1996. The survey area extends from the Egersund Basin and Else Graben to the west and eastward to the coast of northern Denmark, southern Norway and western Sweden and covers therefore the northernmost part of both the Skagerrak-Kattegat Platform and the Norwegian-Danish Basin.

New compilations of regional aeromagnetic and gravity data-sets have been carried out within the frame of the SAS-96 project. GEUS, NGU and NPD have aeromagnetic data from the onshore area of Norway and Denmark, as well as on- and offshore gravity data from collaborations with the Norwegian Mapping Authority (SK), Amarok NIASA and the Universities of Oslo and Århus.

A preliminary interpretation was reported in December 1996 (Olesen *et al.* 1996). In the present report we include the following items:

1. Combined interpretations of aeromagnetic, gravity and seismic data along 5 selected regional lines.
2. Production of a top to basement map constrained by aeromagnetic and gravity depth estimates.
3. Detailed studies of the high frequency aeromagnetic anomalies in the Norwegian-Danish Basin.
4. Compilation of regional aeromagnetic and gravity data-sets for the northeastern North Sea, Skagerrak, Kattegat and adjacent land areas.

We have emphasised the interpretation of the Norwegian-Danish Basin since it has been prioritised by the sponsoring petroleum companies.

2 MAIN STRUCTURAL ELEMENTS

Fig. 2.1 shows the main structural elements of the study area (Vejbæk & Britze 1994) covering the Norwegian-Danish Basin, the Skagerrak-Kattegat Platform and the northern part of the Ringkøbing-Fyn High. The main structural elements in the adjacent basement of the Norwegian-Danish Basin are the N-S trending Mandal-Ustaoset Fault Zone (Sigmond 1985) and the NE-SW trending Porsgrunn-Kristiansand Shear Zone (Starmer 1991) in mainland Norway and the N-S trending Dalsland Boundary Fault (Berthelsen 1977) in Bohuslän on mainland Sweden. Two main igneous provinces exist within the area; the Upper Carboniferous - Permian (c. 300-245 Ma) Oslo Graben to the northeast (Ramberg 1976) and the Sveconorwegian (c. 930 Ma) Rogaland Igneous Complex (Duchesne *et al.* 1987) to the northwest. The Oslo Graben is dominated by intermediate and acidic igneous activity and the Rogaland Igneous Complex shows a wide range of intrusions from norites, to anorthosites, granodiorites and granites (Fig. 2.2). The latter complex stretches from 20 km NW of Egersund eastwards to Lindesnes at the southernmost tip of Norway.

The Sorgenfrei-Tornquist Zone is a complex tectonic zone forming the northwestern part of the Tornquist-Teisseyre Lineament, one of the major European tectonic sutures (Liboriussen *et al.* 1987). The Sorgenfrei-Tornquist Zone separates the Skagerrak-Kattegat Platform from the Norwegian-Danish Basin and experienced multiple deformation from Late Ordovician to Tertiary times. It has been argued that its evolution was dominated by tensional tectonics during the Early Palaeozoic and by dextral wrench tectonics during the late Palaeozoic (Liboriussen *et al.* 1987, Mogensen 1994). This latter led to the development of curvilinear faults and the subsidence of rift basins. The main structures bordering the northwestern segment of the Sorgenfrei-Tornquist Zone are the Børglum Fault to the northeast and the Fjerritslev Trough and the Bulberg Block to the southwest. The formation of the Permo-Carboniferous Oslo Rift system (incl. the Skagerrak Graben and the Oslo Graben) to the northeast represents a reactivation of a Sveconorwegian structure and is closely linked to the dextral strike-slip movements along the Sorgenfrei-Tornquist Zone (Ro *et al.* 1990, Sundvoll & Larsen 1994, Lie 1995). During the Late Cretaceous and Early Cenozoic dextral transpressive stresses caused the partial inversion of Mesozoic basins associated with the Tornquist-Teisseyre lineament (Pegrum 1984, Mogensen & Jensen 1994). The Norwegian-Danish Basin is to a large extent dominated by salt-related tectonics (Sørensen *et al.* 1992, Vejbæk & Britze 1994). Two major N-S trending faults, the Krabbe and Kreps Fault Zones (Brekke *et al.* 1989, Vejbæk & Britze 1994) down-throw rocks on their western sides (approximately 0.5-1.0 km offset at top pre-Zechstein level) in the western Norwegian-Danish Basin.

A depth to magnetic basement of 8-12 km in the Norwegian-Danish Basin has earlier been interpreted by Hospers & Rathore (1984). The depth of the Farsund Basin was estimated to 9 km. An estimate of the pre-Zechstein-salt Palaeozoic sediments reveals a thickness in excess of

4 km in the central parts of the Norwegian-Danish Basin and the Farsund Basin and less than 2 km in the basement high areas (Hospers *et al.* 1986).

3 DATA-SETS

3.1 Aeromagnetic data

The SAS-96 survey was flown with a line spacing of 2 km and a tie-line separation of 5 km (Fig. 3.1) and is described by Olesen *et al.* (1996). Line and tie-line directions are 135°/315° and 225°/45° respectively. A total of 43.000 km were flown covering an area of approximately 60.000 km^2. The nominal flight altitude was 200 metres and the towed bird was located 60 metres below the aircraft (i.e. 140 m a.s.l.). A cesium vapour (Scintrex MEP 410) magnetometer was applied in the data acquisition. The noise envelope was within ±0.1 nT and most of the data were within the limits of ±0.04 nT. Real time differential GPS navigation with a minimum of 4 satellites was used throughout the survey, resulting in an navigation accuracy better than ±15 m.

The processing of the aeromagnetic data was undertaken using software developed by Geosoft, Ltd. (Geosoft 1995b,1996). The steps in the processing procedure are described by Olesen *et al.* (1996). The large magnetic field produced by the DC power cables between Norway and Denmark tested the levelling algorithms to its limit. The large magnetic fields made accurate levelling in the vicinity of the cables difficult and time-consuming. The 1995 International Geomagnetic Reference Field (IGRF-95) was subtracted from the total field.

A total of four other aeromagnetic surveys have been compiled with the SAS-96 data-set (Table 3.1). The Swedish data from the Bohuslän area were acquired by SGU. We have performed an upward continuation from 30 to 150 metres and resampled the grid from 200mx200m to 500mx500m cells. The aeromagnetic data from northern and central Jutland were acquired in 1965 by Fairey Surveys Ltd. on contract for Dansk Undergrunds Consortium and Gulf Oil Company of Denmark. The hand-contoured maps were digitised by GEUS within the frame of the present project and gridded to a 500mx500m grid. The Kattegat aeromagnetic data had previously been digitised to a 4x4 km grid by the European Geotraverse Project and the data-set was provided to us by the Geological Survey of Sweden (SGU). Manually drawn aeromagnetic contour maps at a scale of 1:50,000 of mainland Norway have earlier been digitised into a 500x500m matrix and the Definite Geomagnetic Reference Field 1965 has been subtracted (Nor. geol. unders. 1992). Most of this area was flown at 150 m flight altitude and a line spacing of 500 metres. The mountainous part of northern Rogaland and Setesdalen was flown at an altitude of 300 m and a line spacing of 1000 m due to more rough topography. Specifications for the different sub-areas are given in Table 3.1. The grids were merged with the SAS-96 data

using a minimum curvature algorithm, GRIDSTITCH, developed by Desmond Fitzgerald and Associates (1996).

Table 3.1 Aeromagnetic surveys compiled for the present project (Map sheet C1 & Fig. 4.1). a.g. - above ground, a.m.s.l. - above mean sea level

Year	Contractor	Area	Flight altitude	Line spacing	Tie-line spacing	Recording
1996	NGU	Skagerrak-North Sea (SAS-96)	140 m a.m.s.l.	2 km	5 km	digital
1959-71	NGU	Southern Norway	150-300 m a.g.	500-1000 m	--	analogue
1969-93	SGU	Bohuslän	30 m a.g.	200 "	--	analogue-digital
1965	Hunting Surveys	Northern Jutland	750 m a.m.s.l.	3-6 km	12 km	analogue
1970-71	Fairey Surveys	Kattegat	600 m a.m.s.l.	4 km	20-30 km	"

3.2 Gravity data

The present study is based on measurements from 5400 gravity stations (Table 3.2) on land collected by NGU, GEUS, SGU, SK (Norwegian Mapping Authority), Ramberg (1976), Balling & Falkum (1975) and Lind & Saxov (1970) and approximately 40,000 km of marine gravity profiles (Fig. 4.2) collected by the Norwegian Petroleum Directorate, Mobil Exploration, Statoil and the Norwegian Mapping Authority. The marine data-sets were compiled and levelled by Amarok NIASA. The complete Bouguer reduction of the gravity data was computed using a rock density of 2670 kg/m^3 on mainland Norway and 2000 kg/m^3 on mainland Denmark. The spacing between the gravity stations varies in most of the on land area between 1 and 3 km. Gravity data in the northern Jutland area was digitised from hand-contoured maps because these older maps are based on a denser net of measurements than the modern digital data-set. A simple Bouguer correction was carried out on gravity measurements on the sea using a density of 2200 kg/m^3. The International Gravity Standardisation Net 1971 (I.G.S.N. 71) and the Gravity Formula 1980 for normal gravity were used to level the surveys. The reference system for the Danish on-land gravity data was not known. Modern gravity data from the Geodetic Institute in Denmark were gridded and subtracted from the digitised data to find the average difference (11.0 mGal) from the I.G.S.N.71. The data-set was interpolated to a square grid of 2 km x 2 km using the minimum curvature method (Swain 1976, Geosoft 1996). A Bouguer anomaly map at the scale of 1:500,000 (Map C2, Fig. 4.2) was produced from this grid using the map production system of Geosoft (1996). The locations of the gravity profiles

are shown on the map. A Bouguer gravity map (Fig. 4.5) of the western area was also presented in the SAS-96, Report Part I (Map 6, Olesen *et al.* 1996).

Table 3.2 Gravity data from NGU, GEUS, SGU, SK (Norwegian Mapping Authority), Ramberg (1976), Balling & Falkum (1975) and Lind & Saxov (1970) and Smithson (1963) compiled in the present project (Map C2, Fig. 4.2).

Area	No.	Institution.	Reference
Bohuslän	267	Geological Survey of Sweden (SGU)	
Bohuslän	662	Swedish Mapping Authority (LMV)	
Southern Norway	581	Norwegian Mapping Authority (SK)	.
Østfold	1061	University of Århus	Lind & Saxov 1970
Oslo Region	356	University of Oslo	Ramberg 1976
Arendal and Jæren	663	Geological Survey of Norway (NGU)	Sindre 1993
Grimstad and Herefoss	173	University of Oslo	Smithson 1963
Agder	1637	University of Århus	Balling & Falkum 1975

3.3 Petrophysical data

Some of the magnetic and gravimetric anomalies within the project area are continuous from land onto the continental shelf. It is therefore important to know the density and magnetic properties of the rocks on land when interpreting potential field data covering offshore areas. NGU has earlier carried out petrophysical sampling programmes (for density, susceptibility and remanence measurements) in the Arendal and Egersund areas (Sindre 1992, McEnroe *et al.* 1996). Rock density studies from the nearby mainland, collected during geological mapping and geophysical studies, have earlier been published by other geophysicists interpreting gravity data (Smithson 1963, Lind 1967, Smithson & Barth 1967, Lind & Saxov 1970, Ramberg & Smithson 1971, Balling & Falkum 1975, Ramberg 1976 and Smithson & Ramberg 1979) Previous petrophysical studies have also documented that the Permian volcanics within the Oslo Region are highly magnetic (Thorning & Abrahamsen 1980, Åm & Oftedahl 1977). The NRM-directions as measured by Thorning & Abrahamsen (1980) and Torsvik (in prep.) are partly dominated by a viscous component (close to the present earth field direction) and by a flatlying, slightly negative Permian direction (Table 3.3). NRM-directions from the Sveconorwegian Rogaland Igneous Complex do also show negative inclination, but are steeper than the Permian direction (Table 3.3 and Fig. 3.2).

Table 3.3 Magnetic properties of Permian and Proterozoic rocks from the survey area (Åm & Oftedahl 1977, Thomassen 1971, Thorning & Abrahamsen 1980 and McEnroe *et al.* 1996).

Rock type	Location	No.	Suscept.	Q-value	NRM Dec., Inc.	Reference
Diabase	Bohuslän	6	0.068	0.66	181,-6 (n=5) 264,81 (n=1)	Thorning & Abrahamsen 1980
Diabase	Tvedestrand	15	0.015	2.74	216,-27(n=15)	Torsvik in prep.
Basalt	Øyangen/Oppkuven	19	0.041	0.9		Åm & Oftedahl 1977
Basalt	Krokskogen	11	0.020	2.0		Åm & Oftedahl 1977
Basalt	Nittedalen	25	0.060	1.2		Åm & Oftedahl 1977
Basalt	Alnsjøen	22	0.048	4.0		Åm & Oftedahl 1977
Basalt	Bærum	20	0.072	0.3		Åm & Oftedahl 1977
Basalt	Glitrevatn	15	0.062	1.2		Åm & Oftedahl 1977
Basalt	Vestfold	42	0.067	0.8		Åm & Oftedahl 1977
Basalt	Skien	60	0.109	1.3		Åm & Oftedahl 1977
Norite	Tellnes, Rogaland	191	0.037	7.3	293,-64 (n=32)	McEnroe *et al.* 1996

As constraints for the gravity modelling we have used information from ten petroleum exploration wells in the Danish sector of the Norwegian-Danish Basin. The densities of sedimentary sequences calculated from density logs are shown in Table 3.4. The average values were used to constrain 2½D modelling along profiles SKAG-86-02, SKAG-86-03, SKAG-86-05, SKAG-86-07 and SKAG-86-18. The incorporation of petrophysical data leads to more precise quantitative analysis, and reduces the inherent ambiguity in the interpretation of the aeromagnetic data.

Table 3.4 **Density of sedimentary sequences from density logs of wells in the Norwegian-Danish Basin. The estimates (*1000kg/m^3) are used for gravity modelling along profiles SKAG02, SKAG03, SKAG05, SKAG07, and SKAG18. Numbers in parentheses show depth in metres to the base of the different sequences.**

Well No. Operator Year Structure Name	L-1 Chevron 1970 Else	D-1 Gulf 1968 Jane	Ibenholt-1 Phillips 1987 Ibenholt	R-1 Chevron 1973 Kaye	Inez-1 Chevron 1977 Inez	F-1 Gulf 1968 Nina	K-1 Chevron 1970 Lena	C-1 Gulf 1968 Dora	Felicia-1 Statoil 1987 Felicia	J-1 Gulf 1970 Lisa	Density adapted for modelling
Water depth	55m	49m	40m	37m	35m	41m	56m	27m	69m	44m	1.03
Start of log	1179m	695m	1134m	1041m	1023m	755	957m	1130m	120m	1026m	
Pleistocene											
Post Chalk Goup	2.16 (2015)	2.06 (1205)	2.10 (1447)								2.15
Chalk Group	2.54 (2316)	2.47 (1462)	2.47 (1641)	2.24 (-1180)	2.43 (-1250)	2.28 (1283)	--	--	2.25 (712)		2.45
Lower Cretaceous	2.47 (2377)	2.29 (1511)	2.37 (1701)	2.30 (1262)	2.25 (1394)	2.23 (1511)	2.29 (1240)	2.27 (1286)	2.14 (905)		2.35
Jurassic	2.39 (2416)	2.23 (1543)	2.27 (1749)	2.35 (1303)	2.30 (1633)	2.33 (2041)	2.33 (1947)	2.18 (1373)	??1.79 (1505)	2.41(-1697)	2.35
Triassic	2.45 (2455)	2.41 (1687)	2.39 (1954)	2.29 (1998)	2.30 (1949+)	2.39 (2384+)	2.28 (2256+)	2.36 (2529)	2.42 (4695)	2.35 (1952+)	2.40
Zechstein Group, salt	2.86 (2553)	2.12 (3321)	2.06 (2141)	-				2.08 (3034)	2.01 (5057)		2.05
Zechstein Gr., dolomite			2.80 (2491)					2.75 (3161)	2.67 (5134)		2.75
Rotliegende Group	2.67 (2671+)	2.46 (3528+)	2.38 (2533)	2.49 (2676+)				2.59 (3171+)	2.64 (5290)		2.60
Cambro-Silurian											2.78*
Precambrian basement			2.63(2558+)								2.73**
Mantle											3.30

*Density data from the Cambro-Silurian of the Oslo Region (31 samples, Ramberg 1976).

**Density data from the mainland Norway and Sweden (See Table 3.5) are included in the calculation of the mean basement density.

Published density data (Table 3.5) of basement rocks from the coastal area of southern Norway and western Sweden (Bohuslän) have been compiled for the present project. Representative rocks units (mainly gneisses) are selected from the area. Density data from the Rogaland Igneous Complex and the Herefoss, Grimstad and Iddefjord Granite Complexes etc. are excluded in the estimate of the general basement density. The 'normal' density of the Precambrian basement below the Norwegian-Danish Basin is estimated to 2730 kg/m^3.

Table 3.5 Density of basement rocks from the coastal area of southern Norway and western Sweden (Bohuslän). Representative rock units are selected from the area. Density data from the Egersund Anorthosite Province and the Herefoss, Grimstad and Iddefjord Granite Complexes etc. are excluded in the compilation of the 'normal' density of the Precambrian basement.

Location	Rock type	No.	Density (kg/m^3)	Reference
Egersund area	Gneiss	N/A	2700	Smithson & Ramberg 1979
Flekkefjord area	Gneiss	287	2690	Balling & Falkum 1975
Mandal area	Gneiss	37	2730	Smithson & Barth 1967
Telemark area	Gneiss etc.	36	2760	Smithson 1963
Bamle	Gneiss etc.	54	2810	Smithson 1963
Bamle	Gneiss	166	2734	Sindre 1992
Skien-Gvarv	Gneiss etc.	29	2680	Ramberg 1976
Østfold	Gneiss	42	2660	Lind & Saxov 1970
Østfold	Gneiss	61	2750	Ramberg & Smithson 1971
Bohuslän	Gneiss	20	2730	Lind 1967
Egersund area	Norite	N/A	3000	Smithson & Ramberg 1979
Egersund area	Norite	86	3090	McEnroe *et al.* 1996

4 INTERPRETATION METHODS

4.1 Map production and data enhancement

Regional maps at a scale of 1:500.000 and detailed maps at a scale of 1:250.000 are reported in the SAS-96 Report Part I (Olesen *et al.* 1996) and in the present report (SAS-96 Part II). An overview of the maps is presented in Table 4.1. The present report includes aeromagnetic and gravity compilation maps at a scale of 1:500.000 (Maps C1 & C2) and four 1: 250.000 scale maps from the eastern area and a 1:250.000 interpretation map of the western area. The two former maps include data from the adjacent areas of mainland Denmark, Norway and Sweden and the Kattegat area and are shown on a reduced scale in Figs. 4.1 & 4.2. Two of the aeromagnetic maps from the western area are also shown at a reduced scale in the present report.

Enhancement techniques akin to those commonly used in image processing were applied to the aeromagnetic and gravity data, along with the more traditional geophysical post-processing enhancements. Histogram-equalisation, high-frequency filtering and shaded-relief presentation have been used as standard techniques in the map production. Shaded-relief presentations, which treat the grid as topography illuminated from a particular direction, have the property of enhancing lineaments which lie oblique to the direction of illumination.

The magnetic total field referred to IGRF 1995 is shown at a scale of 1:500.000 and 1:250.000 in Maps 1 and 2 in the SAS-96 Report Part I. Map sheet E1 shows the equivalent 1:250.000 map of the eastern area. A frequency filtered grid using a Butterworth roll-off filter (Geosoft 1994a) revealing anomalies with wavelengths less than 6 km is displayed as a grey-tone shaded relief image on top of the coloured 1:250.000 total field map (Maps 2 and E1, Fig. 4.3). To enhance the high frequency component of the high resolution SAS-96 survey, a shaded relief image of the high-pass component of the grid is also presented in colour (Maps 4 & E3). Maps of stacked high-pass Butterworth filtered (6 km cutoff) profiles (Maps 3 and E2) were produced to show the shape of individual high frequency anomalies to help in estimating the dip and depth of the sources of the anomalies. The analytic signal (amplitude of the total magnetic gradient) of the western and eastern areas is displayed as a shaded relief image in Maps 5 (Fig. 4.4) and E4, respectively. The 2-D frequency domain processing was carried out using software by Geosoft (1994a). The top pre-Zechstein faults, salt diapirs and salt pillows from the interpretation of Vejbæk and Britze (1994) are included on the map sheets, as are the locations and depths of exploration wells.

Table 4.1 **Total list of produced maps in the SAS-96 Project. *Report I* - NGU Report 96.149 (SAS-96 Report Part I), *Report II* - NGU Report 97.022 (SAS-96 Report Part II; present report). All the maps (except the stacked profile maps) are presented as shaded relief.**

Area	Map type	Scale	Map no. and Report no	Figure no. (reduced scale)
SAS-96 area	Mag. total field + high pass	500.000	Map 1, Report I	Fig. 3, Report I
SW Scandinavia	Mag. total field	500.000	Map C1, Report II	Fig. 4.1, Report II
SW Scandinavia	Bouguer gravity	500.000	Map C2, Report II	Fig. 4.2, Report II
Western SAS area	Mag. total field + high pass	250.000	Map 2, Report I	Fig. 4, Report I Fig. 4.3, Report II
Western SAS area	Mag. stacked profiles, high-pass 6, km cutoff	250.000	Map 3, Report I	Fig. 5, Report I
Western SAS area	Mag. high pass filtered, 6 km cutoff	250.000	Map 4, Report I	Fig. 6, Report I
Western SAS area	Mag. analytic signal	250.000	Map 5, Report I	Fig. 7, Report I Fig. 4.4, Report II
Western SAS area	Bouguer gravity	250.000	Map 6, Report I	Fig. 8, Report I
Western SAS area	Interpretation	250.000	Map 7, Report I	Fig. 9, Report I Fig. 5.7, Report II
Western SAS area	Depth to basement	250.000	Map W1, Report II	Fig. 5.8, Report II
Eastern SAS area	Mag. Total field + high pass	250.000	Map E1, Report II	
Eastern SAS area	Mag. stacked profiles, high-pass 6 km cutoff	250.000	Map E2, Report II	
Eastern SAS area	Mag. high pass filtered, 6 km cutoff	250.000	Map E3, Report II	
Eastern SAS area	Analytic signal	250.000	Map E4, Report II	

4.2 Depth to magnetic basement

The Euler 3-D deconvolution (Reid *et al.* 1990, Geosoft 1994b) and the autocorrelation methods (Phillips 1975, 1979) were used to estimate the depth to magnetic basement rocks. The interpretation methods are also described in the SAS-96 Part I Report (Olesen *et al.* 1996) but are included in the present report to make a more complete interpretation report. Euler's homogeneity equation relates the potential field (either magnetic or gravity) and its orthogonal

components to the location of the source, given an assumed rate of change of the field with distance. This rate of change (degree of homogeneity) can be interpreted as a structural index (Thompson 1982) describing the form of the source structure as follows:

Table 4.2 Structural indices for Euler 3-D deconvolution.

Structural index	Structure (Magnetic field)	Structure (Gravity field)
0.0	contact	dyke/sill/step*
0.5	thick step*	ribbon
1.0	dyke/sill	pipe
2.0	pipe	sphere
3.0	sphere	-------

* structures found to be most appropriate

The method has the advantages of being applicable to anomalies caused by a wide variety of geological structures and independent of remanent magnetisation and ambient field direction.

The 3-D Euler deconvolution method requires gridded potential field data as input. The method, therefore, depends on the faithfulness of the grid in describing the true spatial variation in the magnetic or gravity field. The SAS-96 grid based on 2 km spaced profiles were of sufficient quality to yield reliable depths in excess of about 2 km. A zeroth order levelled grid was used for the computation of the Euler depth estimates.

We chose to compute Euler depth solutions for two types of source structure; (1) a 'contact' type model where magnetic and non-magnetic materials are juxtaposed on a continuous planar surface and (2) a 'thick step' model where the surface of contact between magnetic and non-magnetic rocks is step-shaped. We set strict rejection criteria when calculating depths which left us with 24,239 solutions for the 'contact' model and 23,825 for the 'thick step' model. These being too many to interpret manually we subjected the data sets to a secondary phase of computer filtering which simulates the selection procedure employed by an experienced geophysicist. Two similar filters were applied as follows:

(1) *The Standard Deviation Filter* - which attempts to minimise the standard deviation of neighbouring depth estimates by identifying and removing inconsistent results (either clearly deeper or shallower than the majority of nearby results). This filtration preserves the spatial focusing of depth estimates along linear source structures.

(2) *The Median Filter* - which removes data in dense areas only. Outlying data are removed until the number of depth estimates per square kilometre falls to a user specified limit. The geographic focusing of depth estimates is lost however the surviving data, because of their reduced spatial density, are easy to display on a map.

Result of filtering

	Data Before	*Data After Filter 1*	*Data After Filter 2*
'Contact':	24,239	2,697	2,144
'Thick Step':	23,825	2,913	2,201

It is notable that both filters, although operating in different ways, reduced the 'contact' and 'thick step' data sets to similar-sized sub-sets containing many of the same data. This is good evidence that the filters were stable and functioned well, a conclusion borne out by manual control of selected parts of the data sets.

We rejected all data which did not survive either of the two selection procedures outlined above (approximately 90% of the original data sets). We assigned unit weight reliability to all surviving depth estimates, and designated depth estimates which survived both selection procedures 'key' depth estimates.

The depth estimates were plotted on the maps of the total magnetic field referred to IGRF-95 (Map 2, Fig. 4.3), Bouguer gravity field (Map 6, Fig. 4.5) and geophysical interpretation maps (Map7, & W1, Figs. 5.7 & 5.8). Comparisons with results from drilling (see section 5.2 below) indicate that the structural index of 0.5 is the most appropriate to apply in this tectonic setting. This observation is also in agreement with experiences from other areas (Reid *et al.* 1990, Olesen & Smethurst 1995).

The autocorrelation algorithm (Phillips 1975, 1979) was also used to estimate the depth to magnetic basement rocks. The computer implementation of this method of Torsvik & Olesen (1992) was used. The magnetic basement is defined as a two-dimensional surface constructed from a large number of very thin vertical 'dykes' of differing magnetisation. The method assumes that every one of the 'dykes' extends to infinity in directions perpendicular to the profile, as well as vertically downwards. The upper termination of the 'dykes' is the basement surface. This depth can vary from 'dyke' to 'dyke'. The 'dykes' placed next to one another together define the topography of the magnetic basement surface. The depth to this surface is estimated by passing a short window along the magnetic profile, estimating a depth for each position of the window. A total of 80 autocorrelation depth estimates are plotted on Maps 2, 6, 7 and W1 (Figs. 4.3, 4.5, 5.7 & 5.8).

The depth can be estimated from a value of the single autocorrelation at a single lag (Phillips 1975, 1979). In practice the first lag (n=1) is used to estimate depth, while higher lags (n=2,3,4) are used to check the validity of the estimate. A second solution can be expressed in terms of the autocorrelation at two successive lags. Sources at different depths can be separated using this formula, i.e. anomalies caused by deep and shallow bodies in the same profile.

4.3 Forward modelling

We have carried out forward modelling of the gravity field along four seismic profiles across the Norwegian-Danish Basin, each of the profiles consists of two seismic lines SKAG-86-02 and RTD-81-11, SKAG-86-03 and RTD-81-10, SKAG-86-05 and RTD-81-08, SKAG-86-07 and RTD-81-06 (Figs. 5.1-5.5). A fifth profile (NDT96-301 and SKAG86-18) is a tie-line (Fig. 5.8) perpendicular to the other four profiles. Magnetic modelling was carried out along the SKAG-86-07 line. (Figs. 5.4-5.5). When computing the response from the model we have used the new Windows NT version of the IMP computer program of Torsvik (1992). The basic model in this program comprises 2½ dimensional bodies, i.e. bodies of polygonal cross-section of finite length in the strike direction.

Constraints offered by seismic information have been used. Seismic interpretations were digitised and depth-converted using the interval stacking velocities (Table 4.3) from the seismic sections. The depth-converted seismic horizons were imported directly into the IMP programme package. The depth estimates obtained from the autocorrelation and Euler methods were also used to constrain the models.

Table 4.3 Interval stacking velocities (*1000 m/s) from the seismic sections applied in depth conversion of seismic profiles.

Profile / Unit	SKAG-86-02 RTD-81-11	SKAG-86-03 RTD-81-10	SKAG-86-05 RTD-81-08	SKAG-86-07 RTD-81-06	NDT96-301 SKAG86-18
Sea water	1.48	1.48	1.48	1.48	1.48
Pleistocene	1.7	1.7	1.8	1.8	1.8
Post Chalk Group	2.3	2.1	1.9	1.9	2.1
Chalk Group	3.6	4.0	3.3	3.3	4.0
Lower Cret.-Jur.	3.0	2.9	2.8	2.8	3.0
Triassic	4.5	5.0	4.5	4.5	5.0
Zechstein Group		4.6	4.6	4.6	4.6

Forward modelling of the sand channels (Fig. 5.10) was carried out utilising an algorithm to calculate the magnetic response of prism-shaped bodies with arbitrary polarisation by Bhattacharyya (1964).

4.4 Geophysical interpretation maps

A structural interpretation map with depth to magnetic basement estimates was presented in Maps 7 and W1 (Figs. 5.7 and 5.8). Locations and numbers of individual depth estimates from both the Phillips autocorrelation and Euler methods were plotted. The interpretation of the depth estimates was carried out by interpolation and contouring. High frequency anomalies interpreted to represent magnetic volcanics in the area to the north of the Ringkøbing-Fyn High are excluded from the basement model. Hand-drawn depth contours were digitised and then interpolated to a regular grid using the minimum curvature method with a tension factor of 0.5 (Map W1 and Fig. 5.8). The filtered depth estimates (see section 4.2) are plotted on Map W1 (Fig. 5.8) in order to demonstrate the foundation in data for the interpretation.

The aeromagnetic anomalies are classified according to the most likely source. Regional fault zones interpreted from aeromagnetic and gravity data and two areas of negative magnetic anomalies offshore from the Egersund anorthosite and the Lyngdal granite (which both belong to the Rogaland Igneous Complex , Fig. 2.2) are plotted.

The top pre-Zeichstein faults interpretation of Vejbæk and Britze (1994) are included on the map sheet, as are the locations and depths of exploration wells.

5 INTERPRETATION AND DISCUSSION

The magnetic anomaly pattern is interpreted to reflect three different types of magnetic sources; A) Magnetic basement below the Norwegian-Danish Basin and the Kattegat Platform continuing from mainland Norway and Sweden. B) buried Permian volcanic rocks C) High frequency anomalies, buried sand channels of Quaternary age. Type A, B and C anomalies are described and discussed in sections 5.2, 5.3 & 5.4..

5.1 General aeromagnetic and gravity features

The long wave-length component of the Bouguer gravity field (Maps C2 and 6, Figs. 4.2 & 4.5) can be partly interpreted in terms of a Moho topography (Figs. 5.1-5.6). A density contrast of 570 kg/m^3 between the lower crust and mantle is assumed (densities of 2730 kg/m^3 and 3300 kg/m^3 respectively. The Moho depth is adapted from Kinck *et al.* (1991) and applied in the forward modelling of the five interpretation profiles. The Moho depth is shallowest below the central part of the Norwegian-Danish Basin (29 km) and the Skagerrak Graben - Fjerritslev Trough (26-28 km) in the eastern part of the study area. The Moho gets successively deeper towards the Farsund Basin and the mainland of Norway to the north (31-32 km) and towards the Ringkøbing-Fyn High in the south (32 km).

The positive gravity effect from the shallow Moho below the Norwegian-Danish Basin is, however, not sufficient to compensate for the highly reduced gravity effect from the light sediments within the basin. There is a need to introduce more dense material at depth in the crust below the basin. We have chosen to add a body of mafic rock immediately above the Moho. The thickness varies between 3 and 9 km and the width between 80 and 100 km. It is thickest below the deepest part of the Norwegian-Danish Basin on the westernmost interpretation profiles SKAG-86-02 and SKAG-86-03 and thins successively towards the east where it is c. 3 km on the easternmost profile (SKAG-86-07). A similar deep-seated dense mafic rock unit and shallow Moho is included in the gravity model of the Oslo Graben by Ramberg (1976) and Skagerrak Graben by Ramberg & Smithson (1975). An alternative model is to modify the Moho depth interpreted by Kinck *et al.* (1991) to make it shallower below the Norwegian-Danish Basin and deeper below the Sorgenfrei-Tornquist Zone as suggested by Lie & Andersson (1995). By introducing a mafic body above the Moho there is no need to modify the Moho depth and this model is consistent with the crustal model for the Oslo Graben to the north. Reinterpretations of the Oslo Graben gravity high by Wessel & Husebye (1987) suggest that a dense body is most likely located in the upper part of the lower crust and extends eastwards well outside the graben. The inherent ambiguity of the gravity method makes it, however, difficult to decide which of the two models is the correct one. A similar coinciding shallow Moho and dense mafic body in the upper part of the deep crust is also applied to model the Silkeborg gravity high in central Jutland

(Map C2, Figs. 3.1-4.2) by Thybo & Schönharting (1991). Both the Silkeborg and the Oslo Graben gravity highs are interpreted to be related to Permo-Carboniferous igneous activity (Ramberg 1976, Berthelsen 1992). From the new compilation of aeromagnetic data (Map C1) there is evidence that the magnetic anomalies associated with the Silkeborg Gravity High in central Jutland are continuous across the Kattegat to the mainland of Sweden. This observation contradicts the interpretation by Thybo & Schönharting (1989) that these aeromagnetic anomalies in central Jutland are caused by Permian volcanics in the deeper parts of the Norwegian-Danish Basin.

By increasing the density of the consolidated deep sediments of the Norwegian-Danish Basin the size of the mafic body at depth will be reduced but can not be excluded. Some of the wells in the Danish sector are quite deep and provide information of the consolidated part of the stratigraphy. The average density of the Triassic sediments between 1505 m and 4695 m in the Felicia-1 well is for instance 2420 kg/m^3 while the applied density of the Triassic in the modelling is 2400 kg/m^3.

The aeromagnetic anomalies associated with the basement of the Norwegian-Danish Basin is continuous with the aeromagnetic anomalies on mainland Norway indicating that they are caused by Sveconorweian intra-basement sources rather than Permian (or younger) intrusives/extrusives.

5.2 Basement anomalies

The regional basement-related anomalies lie parallel to the Caledonian trend to the northwest as well as to the principal direction of the Precambrian structures to the east. Granulite-facies metamorphic rocks along the coast of Sørlandet are magnetite-bearing (Sindre 1992) and cause magnetic anomalies that can be traced below the offshore Palaeozoic and Mesozoic sediments. The continental-scale Sorgenfrei-Tornquist Zone continues into the SAS-96 area and partly determines the extent of the aeromagnetic and gravity anomalies.

Two of the most prominent anomalies on Maps C1 & 2 (Figs. 4.1 & 4.3) correspond to the continuation of the Rogaland Igneous Complex (negative magnetisation) and the Postorogenic Sveconorwegian belt of granites along the Late Proterozoic Mandal-Ustaoset Fault Zone (MUFZ). The aeromagnetic data indicate that the belt of magnetic Precambrian granites along the MUFZ continues below the Farsund Basin where it seems to be dextrally offset by approximately 10 km along the Sorgenfrei-Tornquist Zone. This constitutes the accumulated offset during several deformation periods from the Palaeozoic to the present. This observation suggests that the more recent interpretation of 15-20 km dextral displacement along the Sorgenfrei-Tornquist Zone since the Early Palaeozoic (Mogensen 1994) is more likely than the

earlier interpretation of approximately 350 km dextral displacement (Pegrum 1984). A relatively minor lateral offset along the Sorgenfrei-Tornquist Zone is also supported by the aeromagnetic data in the Kattegat-northern Jutland area (Map C1, Fig. 4.1) where the NE-SW trending aeromagnetic anomalies from mainland Sweden are continuous across the zone.

The offshore Late Palaeozoic and Mesozoic structures seem partly to have been governed by the older structures. The Kreps Fault Zone (Brekke *et al.* 1989, Vejbæk & Britze 1994) for instance coincides with the eastern border of the N-S trending belt of Postorogenic granites (1000-800 Ma) along the MUFZ (Sigmond 1985). The central section of the N-S trending Krabbe Fault Zone (Vejbæk & Britze 1994) coincides with a large gravity anomaly suggesting that the structure has a deep seated element. The contours of the depth to basement (Map W1) trend partly N-S in the central parts of the Norwegian-Danish Basin supporting this observation.

The depth to magnetic basement (Fig. 5.8, Map W1) is generally deeper than the estimates published by Sellevoll & Aalstad (1971) but locally somewhat shallower than the estimates by Hospers & Rathore (1984), especially in the Egersund Basin where depths of excess of 11 km are reported by the latter authors. Our estimates show depth of 7-8 km in this area. The depth estimates of the Norwegian-Danish Basin indicate a general depth of 7-8 km in large parts of the basin, which is similar to the estimates by Hospers & Rathore (1984) but deeper than the estimates of 6 km by Sellevoll & Aalstad (1971). Our calculations of the depth of the Farsund Basin are approximately 8 km while Hospers & Rathore (1984) estimate depth in excess of 9 km.

Circular gravity anomalies in the central part of the Norwegian-Danish Basin indicates the existence of dense rocks within the basement. The possibility that these anomalies represent central basement highs as suggested by Olesen *et al.* (1996) is not viable since the largest depths to magnetic basement (7-8 km) seem to coincide with the gravity anomalies. Rather, these circular gravity anomalies most likely represent mafic intrusive or extrusive complexes. The age of these rocks are difficult to estimate; they may be of Precambrian (Sveconorwegian) age as the Rogaland Igneous Complex on mainland Norway or they may be related to the late Palaeozoic or Mesozoic rifting in the Norwegian-Danish Basin. Since they are located on a row along the mid-axis of the basin the latter possibility is plausible. These isolated circular intrusions could represent the initial phase of the formation of an axial dyke along the deepest part of the basin. This is a common feature of deep sedimentary basins due to the extension of the crust (White 1992, Gunn 1997a).

A pronounced set of linear aeromagnetic and gravity anomalies trends along the Farsund Basin and indicates significant involvement of basement faulting along the borders of this basin. Magnetic basement depths between 3 km and 9 km were obtained. The western end of the Farsund Basin shallows rapidly and is broken by E-W trending basement blocks. This

observation is also in agreement with seismic interpretations by Lippard & Lunde (1988). Approximately 3 km of pre-Zechstein sediments exists at depth in the Farsund Basin. The E-W trending basement faults in the northeastern part of this basin (Fig. 5.8, Map W1) seem to determine the extension of the WNW-ESE trending top pre-Zechstein faults by Vejbæk and Britze (1994). The discussion of a Precambrian or a Permian origin of the magnetic anomalies in the Farsund Basin is presented in the next section (5.3).

There is a marked negative gravity anomaly along the northern margin of the Ringkøbing-Fyn High (Map C2, Figs. 4.2 & 4.5). which we interpret as either a belt of light intrusives (e.g. granites) or a basin of Palaeozoic or even Proterozoic sediments (sandstones) below Permian volcanics (Profiles SKAG-86-02 and SKAG-86-03, Fig. 5.1-5.2). The depth to the magnetic basement estimates are generally 3-5 km while a sedimentary basin with a density of 2630 kg/m^3 must extend to a depth of 11-13km below the sea level. The width is approximately 20 km. A granite of similar dimensions within the basement would generate the same type of gravity anomaly.

5.3 Permian volcanics

Wide-spread volcanic activity occurred during Late Palaeozoic time in the Oslo Region (300-245 Ma) and southern North Sea - Skagerrak - Kattegat area (Ziegler 1990). Aeromagnetic anomalies related to Permian magmatic activity prevail in the very north of the survey area (where larvikites from Vestfold continue to the south below northern Skagerrak). The northern area of the Skagerrak Graben has the same low magnetic field (Map C1, Fig. 4.1) as the Precambrian basement on the mainland of Norway indicating that (1) this part of the Oslo Rift is lacking volcanic activity or (2) that the volcanics in the area have low magnetisation. Petrophysical measurements (Thomassen 1971, Åm & Oftedahl 1977, Thorning & Abrahamsen 1980; see Table 3.3) of Permian basalts/diabases from adjacent mainland areas show that these volcanics are generally highly magnetic indicating that possibility (1) is the most likely situation, contradicting Faleide *et al.* (1997) who have proposed a thick sequence of Permian volcanics in the Skagerrak Graben.

It is also possible that the magnetic anomalies along the Fjerritslev Trough (Figs. 2.1, 4.1 & 4.3) in the Skagerrak- northern Jutland and the Silkeborg Gravity High in central Jutland are caused by Permian volcanic rocks as suggested by Madirazza *et al.* (1990). Our estimates of the depth to magnetic sources of the Fjerritslev anomaly vary between 4 and 6 km. The anomaly is, however, located within the disturbance zone from the DC-current cables across Skagerrak from Norway to Denmark. The reliability of the depth estimates is therefore reduced.

Coinciding gravity and aeromagnetic anomalies in the Farsund Basin have been interpreted to originate from contemporaneous intrusion of mafic rocks into the lower crust with mafic volcanic activity at surface similar to the Permian tectonic setting of the Oslo Graben further to the north (Åm 1973). The gravity anomaly of the 'Skagerrak volcano' was interpreted in terms of a dense body extending from the upper crust (1-4 km depth) down to a depth of approximately 15 km.

Previous studies have documented that the Permian volcanics of the Oslo Rift are highly magnetic (Thorning & Abrahamsen 1980, Åm & Oftedahl 1977). The NRM-directions as measured by Thorning & Abrahamsen (1980) and Torsvik (in prep.) are partly dominated by a viscous component and partly by a flatlying Permian remanence direction (Table 3.3). The latter has earlier been interpreted to cause the marked negative anomaly to the south of Kristiansand referred to as the 'Skagerrak Volcano' by Sharma (1970), Sellevoll & Aalstad (1971) and Åm (1973). The evidence for a Tertiary volcanic centre presented by Sharma (1970) and Åm (1973) is, however, not compelling. One of the arguments for a Tertiary volcano in the northwestern part of the Skagerrak area is the distribution of Eocene ashes in northern Jutland (Sharma 1970). Reflection seismic data from the area have shown that the potential volcanics offshore Kristiansand do not penetrate the Mesozoic sediments (K. Berli pers. comm. 1997). Aeromagnetic anomalies offshore Kragerø to the northeast were modelled by Åm (1973) applying a steep, negative Tertiary NRM-direction. Palaeomagnetic dating of ultramafic dykes (damtjernites) outside Kragerø by Storetvedt (1968) giving Tertiary ages was used to support this interpretation. A Rb-Sr isochron age dating (Dahlgren 1994) of this dyke has, however, revealed a Late Proterozoic age (576 Ma). The remanence directions of both the late Proterozoic and Tertiary are, however, both steep (negative or positive) and therefore difficult to distinguish. The Kragerø anomaly can consequently be modelled using a Late Precambrian remanence direction.

The existence of Permian intrusives below the Farsund Basin may also be questioned since the positive aeromagnetic anomalies of the area seem to be continuous with the aeromagnetic anomalies on mainland Norway. The E-W trending, (c. 940 Ma) Lyndal granite (Falkum 1987, Bingen & van Breemen 1996) on mainland Norway is an eastward extension within the Rogaland Igneous Complex and coincides with an E-W trending aeromagnetic anomaly indicating that this direction could also prevail in the Precambrian basement below the Farsund Basin.

Table 5.1 Magnetic properties of Permian and Proterozoic rocks applied in the two models of the SKAG-86-07 profile (Figs. 5.4-5.5). (Modified from Torsvik in prep. and McEnroe *et al.* 1996; see Table 3.3).

Rock type	Age	Suscept.	Rem. int. mA/m	Q-value	NRM Dec., Inc.	Tot. mag. Dec., Inc.
Diabase	Permian	0.027	6500	6.13	216,-30	218,-23
Noritt	Sveconorwegian	0.050	5000	2.55	295,-60	307,-41

The negative magnetic anomaly referred to as the 'Permian Skagerrak Volcano' by earlier authors, may be modelled using a Sveconorwegian NRM-direction (Tables 3.3 & 5.1, Fig 5.5, Profile SKAG-86-07). Fig. 5.4 illustrates the original model using a Permian remanence direction. It is important to notice that the shape of the two bodies are different and that it is also necessary to introduce a low-magnetic part to the north in the model using the Sveconorwegian NRM-direction (Fig. 5.5). The latter model includes a southwards dipping body below the Farsund Basin, while the former shows an almost vertical extension to a depth of 13 km, which is similar to the 15 km deep intrusion by Åm (1976). The neighbouring profile (SKAG-85-05) with a model of the westward extension of the 'Skagerrak volcano'-gravity anomaly reveals a similar model to the Precambrian southward dipping dense body of SKAG-06-07. The magnetisation of this western part of the body is, however, positive. The geological explanation of this enormous body of mafic (or possibly ultramafic) could resemble the residue of the parental magma for the voluminous Rogaland anorthosites. These intrusions and other similar anorthosites around the world are interpretated to be formed from differentiation of a mafic parental magma (Ashwal 1993). The norites within the Rogaland Igneous Complex are, however, of minor volume [up to 4 km deep from gravity modelling by Smithson & Ramberg (1979)] compared with the volumes of the anorthosites. The mafic body below the Farsund Basin is approximately 60km long, 30 km wide and up to 6 km thick and could represent the original mafic residual magma from the anorthosite differentiation.

The partial negative Farsund Basin aeromagnetic anomalies differ from the anomalies of the Oslo Graben which are dominantly positive due to the large intrusive bodies of granites and monzonites. The Oslo Rift basalts and diabases have predominately reversed magnetisation but only in relatively minor volumes and rarely show up on the aeromagnetic map of this area. In the Rogaland Igneous Province, 50 km to the NW of the negative 'Skagerrak Volcano' anomaly there are numerous intrusive bodies revealing reversed magnetisation, predominately anorthosites and norites, Q-values range 0.1-150 (McEnroe *et al.* 1996).

Some of the depth estimates in the Norwegian-Danish Basin are consistent with what is known from exploration drilling. The oval-shaped positive anomaly in the Danish Sector at 5°30'E,

56°25'N yields Euler depth estimates of 3.1 to 3.7 km (Maps 2 & W1) and an exploration well (D-1) located 3 km from the centre of the anomaly has encountered Lower Permian basalts at a depth of 3.508 km (Rasmussen 1974, Nielsen & Japsen 1991). The eruptives make up 18 metres of the deepest part of the hole (total depth 3.526 km) and may therefore be thicker. The Ibenholt-1 well (5°58'E, 56°23' N) 27 km to the east hit Precambrian basement at a depth of 2558 m (Nielsen & Japsen 1991) while the nearest Euler depth estimate show a depth to magnetic basement of 2500 m. These tests show that the chosen Euler structural index of 0.5 (thick step) is appropriate for this type of anomaly.

5.4 Quaternary sand channels

A very distinct set of high frequency NE-SW to ENE-WSW trending anomalies occurs regionally in the southeastern part of the SAS-96 area and is oriented perpendicular to the general trend of the subcropping Tertiary and Mesozoic units (Sigmond 1992). The 5-50 km long curvilinear anomalies terminate towards the Norwegian Channel to the northeast at a water depth between 100 m and 150 m. The study of 3D seismics (Figs. 5.9) from the Siri area in the western part of the SAS-96 area has shown that the anomalies are caused by shallow sand channels. Magnetic modelling (Fig. 5.10) of one of these sand channels (250 m thickness and 2000 m width buried below 100 m of younger sediments) has shown that a susceptibility of $500x10^{-6}$SI is needed to generate a 2 nT amplitude anomaly. Magnetisation along the present earth field is assumed. These channels partly coincide with fault segments along the eastern flank of the Horn Graben and segments of the Krabbe Fault Zone (Figs. 4.4 & 2.1).

The symmetry of the anomaly curves in the stacked profiles plot (Map 3 in SAS-96 Report Part I) and the general NE-SW direction also support that deep incisions cutting into Middle and Upper Pleistocene successions are a likely source of the anomalies. Structures partly coinciding with the aeromagnetic anomalies have been interpreted in the Danish sector of the SAS-96 area from shallow seismic data (Salomonsen 1995, Salomonsen & Albæk Jensen 1994). Equivalent incisions vary in depth from 100 to 350 m and range up to 5 km wide and 25 km long in the mid-North Sea area (Wingfield 1990). The distance between sub-parallel high frequency aeromagnetic anomalies within SAS-96 varies between 2 and 10 km while Ehlers & Linke (1989) found that the average distance between the channels in the Hamburg area was 6 km. The high density of such channels indicates that they mostly formed independently of pre-existing river courses. Salomonsen (1993), however, argue that the channels are partly governed by pre-existing faults and graben-structures. The varying direction of the channels as they appear in the SAS-96 data-set may indicate that they represent channels of different age within the sedimentary column. A study of 3D seismics from the SAS-96 area (Fig. 5.9) does also reveal that at least two different generations of channels exist since one set of channels is cutting another. These sand channels seem to occur widely beneath the northern continental shelf and

lowlands of Europe. The origin of the channels is, however, disputed; Salomonsen (1995) argues that they are the result of intermittent fluvial erosion in relation to glacial periods. Ehlers & Linke (1989) conclude that the channels were eroded by englacial and subglacial meltwater and are consequently the erosive analogues of eskers in areas of soft, deformable bedrock. The channels were infilled by meltwater deposits when the ice sheet melted. By early Saalian time (before 130.000 years b.p.) the channels were completely infilled. Wingfield (1990) believes that the major incisions are the product of a singular mechanism: the outburst of intra-ice-sheet lakes forming jøkulhlaup plunge pools (catastrophic meltwater release) in the marginal parts of the ice sheets. The aeromagnetic method has proved to be an adequate tool for mapping sand channels in the North Sea, as has also been reported from offshore Australia (Gunn 1997b).

Negative aeromagnetic anomalies (Map 2) coincide partly with the salt diapirs and salt pillows interpreted from seismic data by Vejbæk & Britze (1994). This phenomenon is only observable in the magnetic quiet zones, i.e. in the deep sedimentary basins. The negative anomalies are caused by the negative susceptibility of salt and anhydrite, i.e. diamagnetic behaviour (Telford *et al.* 1976). The Siri salt diapir to the southwest of the survey area does seem to have much larger dimensions than interpreted from the seismic data. This observation is also supported by the Bouguer gravity map (Fig. 4.5, Map 6 Olesen *et al.* 1996).

6 CONCLUSIONS

1. The anomaly pattern of the SAS-96 aeromagnetic maps is interpreted to have three different types of magnetic sources A) magnetic basement continuing from the mainland of Norway and Sweden (Sørlandet and Bohuslän) into the Kattegat Platform and the Norwegian-Danish Basin. B) Permian intrusives and volcanics and C) Pleistocene sand channels cutting into substrates of various lithologies.

2. The negative magnetic anomaly attributed to the Permian or Tertiary 'Skagerrak Volcano' by other geophysisists may well be modelled utilising a Sveconorwegian NRM direction. We interpret these coinciding gravity and aeromagnetic anomalies in the Farsund Basin to be an integrated part of the Rogaland Igneous Province continuous from the coast of mainland Norway 50 km to the southwest. This new interpretation may have implications for evaluating the maturation of potential source rocks in the Farsund Basin.

3. Circular gravity anomalies in the central part of the Norwegian-Danish Basin may represent mafic intrusive or extrusive complexes. The age of these rocks are difficult to estimate; they may be of Precambrian (Sveconorwegian) age as the Rogaland Igneous Province on mainland Norway or they may be related to the late Palaeozoic or Mesozoic rifting in the Norwegian-Danish Basin. Since they are located on a row along the mid-axis of the basin the latter possibility is plausible. These isolated circular intrusions could represent the initial phase of the formation of an axial dyke along the deepest part of a syn-rift extensional basin.

4. The depth to magnetic basement estimates indicate a general depth of 7-8 km in large parts of the Norwegian-Danish Basin. Depths between 3 km and 9 km were obtained along the Farsund Basin, and the magnetic anomaly pattern indicates a complex system of fault blocks along the Sorgenfrei-Tornquist Zone. Approximately 3 km of pre-Zechstein sediments exists at depth in the Farsund Basin.

5. The aeromagnetic data indicate that the belt of magnetic Precambrian granites along the Mandal-Ustaoset Fault Zone continues below the Farsund Basin where it seems to be dextrally offset by approximately 10 km along the Sorgenfrei-Tornquist Zone. This constitutes the accumulated offset during several deformation periods from the Palaeozoic to Cenozoic time. A relatively minor lateral offset along the Sorgenfrei-Tornquist Zone is also supported by the aeromagnetic data in the Kattegat-northern Jutland area (Map C1) where the NE-SW trending aeromagnetic anomalies from mainland Sweden are continuous across the zone.

6. A very distinct set of high frequency NE-SW to ENE-WSW trending anomalies occurring regionally in the southeastern part of the SAS-96 area are caused by shallow Pleistocene sand channels (typically of 200-300 m thickness and 2000 m width buried below 100 m of younger

sediments). The 5-50 km long curvilinear anomalies terminate towards the Norwegian Channel to the northeast at a water depth between 100 m and 150 m. The distance between the channels varies between 2 and 10 km. These sand channels seem to occur widely beneath the northern continental shelf and lowlands of Europe. The channels were most likely eroded by englacial and subglacial meltwater and are consequently the erosive analogues of eskers in areas of soft, deformable bedrock. The channels were infilled by meltwater deposits when the ice sheet melted. The aeromagnetic method has proved to be an adequate tool for mapping sand channels in the North Sea.

7. The SAS-96 survey is a state of the art data-set and has revealed several groups of high frequency anomalies not discernible in the old NGU data-sets. This is due to the use of more sensitive magnetometers, closer line spacing, more accurate navigation and improved processing and data presentation. Several of the interpreted structures have not been previously reported to the authors knowledge.

7 ACKNOWLEDGEMENTS

The project was financed by the Geological Survey of Denmark and Greenland (GEUS), Mobil Exploration, Norwegian Petroleum Directorate (NPD), Norsk Hydro, Phillips Petroleum, Statoil and the Geological Survey of Norway (NGU). Oddvar Blokkum, Janusz Koziel, John Olav Mogaard and Stig Rønning (NGU) carried out the airborne data acquisition. Atle Sindre, NGU carried out gravity measurements on land in the Rogaland and Agder areas. Other Norwegian mainland gravity data were provided by the Norwegian Mapping Authority (SK), Ivar Ramberg, Norsk Hydro and Niels Balling and Svend Saxov, University of Århus. Amarok NIASA provided the offshore gravity data-set. Kajsa Hult and Sven Aaro, SGU supplied aeromagnetic and gravity data from the Kattegat and Bohuslän areas, respectively. René Forsberg, Danish Geodetic Institute supplied us with modern gravity data from northern Jutland to calculate the reference field of the digitised 1949 gravity data. Mark Prebish (Mobil Exploration), Harald Elstad and Brian Farrelly (Norsk Hydro), Kristen Berli and Bente Fotland (NPD), Arild Gundersen and Neil Judge (Phillips Petroleum), Olaf Langnes and Roar Heggland (Statoil), Henrik Håbrekke, Suzanne McEnroe and Leif Rise (NGU) gave advice and consultation during the project. Section leader Jan Steinar Rønning critically read the report and made suggestions towards its improvement. To all these persons, companies and institutions we express our sincere thanks.

8 REFERENCES

Åm, K. 1973: Geophysical indications of Permian and Tertiary igneous activity in the Skagerrak. *Nor. geol. unders. 287,* 1-25.

Åm, K. & Oftedahl, C. 1977: Brief comments on some aeromagnetic anomalies in the Oslo Region. In: K.S. Heier (Editor) *The Norwegian Geotraverse Project. A Norwegian contribution to The International Upper Mantle Project and The International Geodynamics Project,* 209-222.

Ashwal, L.D. 1993: Anorthosites. *Springer-Verlag, New York - Berlin.* 422 pp.

Balling, N.P. & Falkum, T. 1975: A combined geophysical and structural-geological investigation of the Precambrian intrusive Homme granite in south-western Norway. *Geol. Fören. Stockh. Förh. 97,* 338-356.

Berthelsen, A. 1977: Tentative tectonic division of the Sveco-Norwegian belt. In: *Field GuideCOMTEC 77 on Tectonics of Precambrian orogens of southern Scandinavia,* Copenhagen.

Berthelsen, A. 1992: From Precambrian to Variscan Europe. In: D. Blundell, R. Freeman & S. Mueller (Editors) *A continent revealed, The European Geotraverse.* Cambridge University Press, Cambridge, 153-164.

Bhattacharyya, B.K. 1964: Magnetic anomalies due to prism-shaped bodies with arbitrary polarization. *Geophysics 29,* 517-531.

Bingen, B. & van Breemen, O. 1996: U-Pb titanite geochronology in Rogaland -Vest Agder (SW Norway): Regional temperature at the time of intrusion of the Rogaland anorthosites. In: D. Demaiffe (Ed.) *Petrology and geochemistry of magmatic suites of rocks in the continental and oceanic crusts. Université Libre de Bruxelles. Royal Museum for Central Africa (Tervuren),* 145-160.

Brekke, H., Færseth, R., Gabrielsen, R., Gowers, M.B. & Pegrum, M. 1989: Nomenclature of tectonic units in the Norwegian North Sea, south of 62°N. – In: *Structural and tectonic modelling and its application to Petroleum geology.* Norwegian Petroleum Society. Abstracts 61.

Dahlgren, S. 1994: Late Proterozoic and Carboniferous ultramafic magmatism of carbonatitic affinity in southern Norway. *Lithos 31,* 141-154.

Desmond Fitzgerald and Associates Pty Ltd. 1996: INTREPID Geophysical Processing and Visualisation Tools Reference Manual Vol. 2, 241 pp.

Duchesne, J.C., Michot, J., Maquil, R., Maijer, C. & Tobi, A.C. 1987: The Rogaland Intrusive Massifs. In: C. Maijer & P. Patget (Eds.) *The geology of southernmost Norway, An excursion guide.* Nor. geol. unders. Spec. Publ. 1, 48-87.

Ehlers, J. & Linke, G. 1989: The origin of deep buried channels of Elsterian age in Nortwest Germany. *Journ. Quatern. Sci. 4,* 255-265.

Faleide, J.I., Myklebust, R., Stuevold, L., Mathisen, G. & Ditcha, E. 1997: Sen-Paleozoisk rifting og magmatisme i Skagerrak, Kattegat og Nordsjøen. *Abstract, 15th Annual Meeting Norwegian Geological Society,* p 34.

Falkum, T. 1987: The Agder migmatitic gneiss complex and post-kinematic granites. In: C. Maijer & P. Patget (Eds.) *The geology of southernmost Norway, An excursion guide.* Nor. geol. unders. Spec. Publ. 1, 34-39.

Geosoft 1994a: MAGMAP, 2-D frequency domain filtering. Users manual. 34 pp.

Geosoft 1994b: GRIDEPTH, 3-D Euler deconvolution of potential field data. Users manual. 29 pp.

Geosoft 1995a: GEOSOFT, Mapping and Processing System (MPS). Users manual. 435 pp.

Geosoft 1995b: OASIS, Data Processing System for Earth Sciences Applications. Users manual. 132 pp.

Geosoft, 1996: OASIS montaj, Data processing system for Earth science applications. Version 4.0 User guide.190 pp.

Gunn, P.J. 1997a: Regional magnetic and gravity responses of extensional sedimentary basins. *AGSO Jour. Austr. Geol. & Geoph. 17,* 115-131.

Gunn, P.J. 1997b: Application of aeromagnetic surveys to sedimentary basin studies. *AGSO Jour. Austr. Geol. & Geoph. 17,* 133-144.

Hospers, J. & Rathore, J.S. 1984: Interpretation of aeromagnetic data from the Norwegian sector of the North Sea. *Geophys. Prospecting 32,* 929-942.

Hospers, J., Rathore, J.S., Jianhua, F. & Finnstrøm, E.G. 1986: Thickness of pre-Zechstein-salt Palaeozoic sediments in the southern part of the Norwegian sector of the North Sea. *Nor. Geol. Tidsskr. 66,* 295-304.

Kinck, J.J., Husebye, E.S. & Lund, C.-E. 1991: The south Scandinavian crust: Structural complexities from seismic reflection and refraction profiling. *Tectonophysics 189,* 117-133.

Liboriussen, J., Ashton, P. & Tygesen, T. 1987: The tectonic evolution of the Fennoscandian Border Zone in Denmark. *Tectonophysics 137,* 21-29.

Lie, J.E. 1995: Deep seismic reflection mapping of crustal and upper mantle structures beneath the Skagerrak Sea, SW Scandinavia. *PhD Thesis, University of Oslo,* 138 pp.

Lie, J.E. & Andersson, M. 1995: The deep seismic image of the crustal structure of the Tornquist Zone beneath the Skagerrak Sea, northwestern Europe. In: *Deep seismic reflection mapping of crustal and upper mantle structures beneath the Skagerrak Sea, SW Scandinavia.* J.E. Lie. PhD Thesis, University of Oslo.

Lind, G. 1967: Gravity measurements over the Bohus Granite in Sweden. *Geol. Fören. Stockh. Förh. 88,* 542-548.

Lind, G. & Saxov, S. 1970: Some geophysical profiles in Østfold. *Nor. geol. unders. 266,* 37-48.

Lippard, S. & Lunde, G. 1988: The geological evolution of the Farsund Sub-basin. *Abstract VI annual TSGS meeting, Institute of Geology, University of Oslo, Internal Report 54,* 3-4.

Madirazza, I., Jacobsen, B.H. & Abrahamsen, N. 1990: Late Triassic tectonic evolution in northwest Jutland, Denmark. *Bull. Geol. Soc. Denmark 38,* 77-84.

McEnroe, S., Robinson, P. & Panish, P. 1996: Rock-magnetic properties, oxide mineralogy and mineral chemistry in relation to aeromagnetic interpretation and search for ilmenite reserves. *NGU Report 96.060,* 153 pp.

Mogensen, T.E. 1994: Palaeozoic structural development along the Tornquist Zone, Kattegat area, Denmark. *Tectonophysics 240,* 191-214.

Mogensen, T.E. & Jensen, L.N. 1994: Cretaceous subsidence and inversion along the Tornquist Zone from Kattegat to the Egersund Basin. *First Break 12,* 211-222.

Nielsen, L.H. & Japsen, P. 1991: Deep wells in Denmark 1935-1990. *Geological Surv. of Denmark Series A 31,* 177 pp.

Norges geologiske undersøkelse 1992: Aeromagnetisk anomalikart, Norge M 1:1 mill, Norges geologiske undersøkelse.

Olesen, O. & Smethurst, M.A. 1995: NAS-94 Interpretation Report, Part III: Combined interpretation of aeromagnetic and gravity data. *NGU Report 95.040,* 50 pp.

Olesen, O., Beard, L. & Smethurst, M.A. 1996: SAS-96 Part I, Skagerrak Aeromagnetic Survey 1996 Processing and Preliminary Interpretation Report *NGU Report 96.149,* 32 pp.

Pegrum, R.M. 1984: The extension of the Tornquist Zone in the Norwegian North Sea. *Nor. Geol. Tidsskr. 64,* 39-68.

Phillips, J.D. 1975: Statistical analysis of magnetic profiles and geomagnetic reversal sequence *Ph.D. thesis. Stanford University,* 134 pp.

Phillips, J.D. 1979: ADEPT: A program to estimate depth to magnetic basement from sample magnetic profiles. *U.S. geol. Surv. open-file report 79-367,* 35 pp.

Ramberg, I.B. 1976: Gravity interpretation of the Oslo Graben and associated igneous rocks. *Nor. geol. unders. Bull. 325,* 194 pp.

Ramberg, I.B. & Smithson, S.B. 1971: Gravity interpretation of the southern Oslo Graben and adjacent Precambrian rocks, Norway. *Tectonophysics 11,* 419-431.

Ramberg, I.B. & Smithson, S.B. 1975: Geophysical interpretation of crustal structure along the southeastern coast of Norway and Skagerrak. *Geol. Soc. Am. Bull. 86,* 769-774.

Rasmussen, L.B. 1974: Some geological results from the first five Danish exploration wells in the North Sea. *Geol. Surv. of Denmark III series 42,* 46 pp.

Reid, A.B., Allsop, J.M., Granser, H., Millett, A.J. & Sommerton, I.W. 1990: Magnetic interpretation in three dimensions using Euler deconvolution, *Geophysics 55,* 80-91.

Ro, H.E., Stuevold, L., Faleide, J.I. & Myhre, A.M. 1990: Skagerrak Graben - the offshore continuation of the Oslo Graben. *Tectonophysics 178,* 1-10.

Salomonsen, I. 1993: Quaternary depositional and drainage systems in the eastern North Sea basin. *PhD Thesis, University of Copenhagen,* Unpublished, 115 pp.

Salomonsen, I. 1995: Origin of a deep buried valley system in Pleistocene deposits of the eastern central North Sea. *Danmarks Geologiske Undersøgelse C 12,* 8-17.

Salomonsen, I. & Albæk Jensen, K. 1994: Quaternary erosional surfaces in the Danish North Sea. *Boreas 23,* 244-253.

Sellevoll, M. A. & Aalstad, I. 1971: Magnetic measurements and seismic profiling in the Skagerrak. *Marine Geophys. Res. 1,* 284-302.

Sharma, P.V. 1970: Geophysical evidence for a buried volcanic mount in the Skagerrak. *Bull. of Geol. Soc. of Denmark 19,* 368-377.

Sigmond, E.M.O. 1985: The Mandal - Ustaoset line, a newly discovered major fault zone in South Norway. In: A.C. Tobi & J.L.R. Touret (Editors) *The deep Proterozoic crust in the north Atlantic provinces,* D. Reidel Publishing Company, 323-331.

Sigmond, E.M.O. 1992: Bedrock map of Norway and adjacent ocean areas. Scale 1:3 million. *Norges geologiske undersøkelse, Trondheim.*

Sindre, A. 1992: Regional tolkning av geofysiske data, kartblad Arendal, M 1:250.000. *NGU Report 92.213,* 30 pp.

Sindre, A. 1993: Tolkning av magnetometri og gravimetri i Skagerrak, kartblad Arendal, M 1:250.000. *NGU Report 93.114,* 11 pp.

Smithson, S.B. 1963: Granite studies: I. A gravity investigation of two Precambrian granites in South Norway. *Nor. geol. unders. 214B,* 53-140.

Smithson, S.B. Barth, T.F.W. 1967: The Precambrian Holum ganite, South Norway. *Nor. Geol. Tidsskr. 47,* 21-56.

Smithson, S.B.& Ramberg, I.B. 1979: Gravity interpretation of the Egersund anorthosite complex, Norway: Its petrological and geothermal significance. *Geol. Soc. Am. Bull. 90,* 199-204.

Starmer, I.C. 1991: The Proterozoic evolution of the Bamle Sector shear belt, southern Norway: correlations across southern Scandinavia and the Grenvillian controversy. *Precamb. Res. 49,* 107-139.

Storetvedt, K.M. 1968: The permanent magnetism of some basic intrusions in the Kragerø archipelago, S. Norway, and its geological implications. *Nor. Geol. Tidsskr. 48,* 153-163.

Sundvoll, B. & Larsen, B.T. 1994: Architecture and early evolution of the Oslo Rift. *Tectonophysics 240,* 173-189.

Swain, C.J. 1976: A Fortran IV program for interpolating irregularly spaced data using the difference equations for minimum curvature. *Computers & Geosciences 1,* 231-240.

Sørensen, S., Morizot, H. & Skottheim, S. 1992: A tectonostratigraphic analysis of the southeast Norwegian North Sea Basin. In: R.M. Larsen, H. Brekke, B.T. Larsen & E. Talleraas (Editors) *Structural and tectonic modelling and its application to petroleum geology.* Norwegian Petroleum Society (NPF), Elsevier, Amsterdam, 19-42.

Telford, W.M., Geldart, L.P., Sheriff, R.E. & Keys, D.A. 1976: Applied Geophysics. *Cambridge University Press, Cambridge.* 860 pp.

Thomassen, T.C. 1971: En magnetisk ertsmineralogisk studie av basaltene i Oslo-feltet. Thesis , Norwegian Institute of Technology, Trondheim, 123 pp.

Thompson, D.T. 1982: EULDPH: A new technique for making computer-assisted depth estimates from magnetic data. *Geophysics 47,* 31-37.

Thorning, L. & Abrahamsen, N. 1980: Palaeomagnetism of Permian multiple intrusion dykes in Bohuslän, SW Sweden. *Geophys. J.R. Astr. Soc 60,* 163-185.

Thybo, H. & Schönharting, G. 1991: Geophysical evidence for Early Permian igneous activity in a transtensional environment, Denmark. *Tectonophysics 189,* 193-208.

Torsvik, T.H. 1992: IMP5 - Interactive modelling of potential field data (Release 5). *NGU Report 92.305.* 75 pp.

Torsvik, T.H. & Olesen, O. 1992: PDEPTH - calculation of depth to magnetic basement from profile data. *NGU Report 92.212,* 26 pp.

Vejbæk, O.V. & Britze, P. 1994: Geological map of Denmark 1:750.000. *Danmarks Geologiske Undersøgelse 45,* 8 pp.

Wessel, P. & Husebye, E.S. 1987: The Oslo Graben gravity high and taphrogenesis. *Tectonophysics 142,* 15-26

White, R.S. 1992: Magmatism during and after continental break-up. In: B.C. Storey, T. Alabaster & R.J. Pankhurst (Editors) *Magmatism and the causes of continental break-up.* Geol. Soc. Soec. Publ. 68, 1-16.

Wingfield, R. 1990: The origin of major incisions within the Pleistocene deposits of the North Sea. *Marine Geology 91,* 31-52.

Ziegler, P.A. 1990: Tectonic and palaeogeographic development of the North Sea rift system. In: D.J. Blundell & A.D. Gibbs (Editors) *Tectonic evolution of the North Sea Rifts.* 1-36, Oxford University Press.

List of figures and maps

Fig. 4.5 Bouguer gravity map (contours and colours) with geophysical interpretations, western area, Map 6 from SAS-96 Report Part I at a reduced scale.

Fig. 5.1 Gravity interpretation along the seismic profile SKAG-86-02 and RTD-81-11 (Figs. 2, 6, 7 and 9, Maps 4, 5 and 9). Applied densities are shown in Table 3.4. Violet colour - mantle.

Fig. 5.2 Gravity interpretation along the seismic profile SKAG-86-03 and RTD-81-10 (Figs. 2, 6, 7 and 9, Maps 4, 5 and 9). Applied densities are shown in Table 3.4. Violet colour - mantle.

Fig. 5.3 Gravity interpretation along the seismic profile SKAG-86-05 and RTD-81-08 (Figs. 2, 6, 7 and 9, Maps 4, 5 and 9). Applied densities are shown in Table 3.4. Violet colour - mantle.

Fig. 5.4 Gravity and magnetic interpretation along the seismic profile SKAG-86-07 and RTD-81-06 (Figs. 2, 6, 7 and 9, Maps 4, 5 and 9). Applied densities and magnetic properties are shown in Tables 3.4 and 5.1, respectively. A Permian NRM direction is applied in the magnetic modelling. Violet colour - mantle.

Fig. 5.5 Gravity and magnetic interpretation along the seismic profile SKAG-86-07 and RTD-81-06 (Figs. 2, 6, 7 and 9, Maps 4, 5 and 9). Applied densities and magnetic properties are shown in Table 3.4 and 5.1, respectively. A Sveconorwegian NRM direction is applied in the magnetic modelling. Violet colour - mantle.

Fig. 5.6 Gravity interpretation along the seismic profile NDT96-301 and SKAG-86-18 (Figs. 2, 6, 7 and 9, Maps 4, 5 and 9). Applied densities are shown in Table 3.4. Violet colour - mantle.

Fig. 5.7 Geophysical interpretation map, western area, Map 7 (SAS-96 Part I Report, Olesen *et al.* 1996) at a reduced scale.

Fig. 5.8 Depth to magnetic basement interpretation map, western area, Map W1 at a reduced scale.

Fig. 5.9 (a) Seismic section and (b) chair diagram from a 3D seismic cube in the Siri area showing Pleistocene sand channels coinciding with high-frequency aeromagnetic anomalies in the SAS-96 area (Figs. 4.3 & 4.4). Shot point distance 12.5 m.

Fig. 5.10 Aeromagnetic modelling of a Pleistocene sand channel from the Siri area applying the algorithm by Bhattacharyya (1964).

Map C1. Total magnetic field anomaly map (contours and colours), Compilation of southwestern Scandinavia, Scale 1:500.000

Map C2. Bouguer gravity map (contours and colours), Compilation of southwestern Scandinavia, Scale 1:500.000

Map W1. Geophysical interpretation map, western SAS-96 area, Scale 1:250.000

Map E1. Total magnetic field anomaly map, (contours and colours) and 6 km high-pass filtered grid as shaded relief, western SAS-96 area, Scale 1:250.000.

Map E2. Stacked profiles, high-pass Butterworth filtered, 6 km cutoff, eastern SAS-96 area, Scale 1:250.000

Map E3. High-pass Butterworth filtered grid (contours and colours), 6 km cutoff, eastern SAS-96 area, Scale 1:250.000

Map E4. Magnetic gradient amplitude map, Analytical signal (contours and grey-tone), western SAS-96 area, Scale 1:250.000

Maps included in the SAS-96 Report, Part I (Olesen *et al.* 1996).

Map 1. Total magnetic field anomaly map, SAS-96 area (contours and colours), Scale 1:500.000

Map 2. Total magnetic field anomaly map (contours and colours), western SAS-96 area, Scale 1:250.000

Map 3. Stacked profiles, high-pass Butterworth filtered, 6 km cutoff, western SAS-96 area, Scale 1:250.000

Map 4. High-pass Butterworth filtered grid (contours and colours), 6 km cutoff, western SAS-96 area, Scale 1:250.000

Map 5. Magnetic gradient amplitude map, Analytical signal (contours and grey-tone), western SAS-96 area, Scale 1:250.000

Map 6. Bouguer gravity map (contours and colours) with geophysical interpretations, western SAS-96 area, Scale 1:250.000

Map 7. Geophysical interpretation map, western SAS-96 area, Scale 1:250.000

Exabyte archive-tape from the Skagerrak Aeromagnetic Survey 1996 (SAS-96)

SAS96A.XYZ is a 42 MB ASCII file containing 6 columns. They are:

column 1	X	East-west coordinate in ED-50
column 2	Y	North-south coordinate in ED-50
column 3	LINE	Line number. Includes tie lines (line >= 3000).
column 4	MAG2	Raw total magnetic field data.
column 5	ANOM1	Channel created from MAG2 after subtraction of IGRF-95. Cultural anomalies have been edited out of ANOM1, including those from the DC power cables.
column 6	LEV2	Final 2nd order tie line leveled channel derived from ANOM1. LEV2 has also had decorrugation filters applied in both survey line and tie line directions. The total magnetic field anomaly map was created from this channel. No data are contained in LEV2 for tie lines (LINE >= 3000).

The file is not divided with line number headers. The columns are continuous.

CAUTION: When gridding survey lines, grid only the lines with line numbers less than 3000. Numbers >= 3000 in channel LINE refer to tie lines. Channel LEV2 contains data only for survey lines. A dummy symbol (*) is in LEV2 at tie lines.

SAS_TF.XYZ, SAS_HP6.XYX, and SAS_AS.XYZ are ASCII files constructed by sampling the levelled total magnetic field grid, the 6-km high pass grid, and the analytic signal grid at 500 meter intervals in X and Y directions. COM_MAG.XYZ and COM_BOUG.XYZ are sampled from the aeromagnetic and Bouguer gravity compilations of southwestern Scandinavia (Map C1, 500x500m grid and Map C2, 2x2km grid, respectively). Each file consists of three columns: X, Y, and grid value.

All the XYZ files can be read free-format, i.e. read(##,*), but if for some reason a formatted read is desirable, the following will work from a Fortran read statement:

For SAS96A.XYZ: F11.1, F11.1, I6, F11.1, F11.2, F11.2

For SAS_TF.XYZ,
SAS_HP.XYZ,
SAS_AS.XYZ:,
COM_MAG.XYZ,
COM_BOUG.XYZ,
F11.0, F11.0, F11.4

Other SAS-96 XYZ files:

DEPTH XYZ	Phillips depths to magnetic basement
DEPTH5 XYZ	Euler depths to magnetic basement
SAS9611 XYZ	Reversely magnetised bodies
SAS9612 XYZ	Regional faults from gravity
SAS9613 XYZ	Regional faults from magnetics
SAS9614 XYZ	Sand channels
HEAVY XYZ	Dense bodies in basement
LIGHT XYZ	Low density bodeis in basement
SAS96BOR XYZ	Perimeter of SAS-96 survey
TOLKPROF XYZ	Interpreted profiles
TPZFAULT XYZ	Fault interpretation of Vejbæk & Britze 1994
WELLDANO XYZ	Wells
BLOCKS32 XYZ	License blocks
BORDER XYZ	Norway-Denmark-Sweden border
ELV32 XYZ	Rivers
KYST32 XYZ	Coastline
RGRENS32 XYZ	Norway-Sweden border
SALTDIAP XYZ	Salt diapirs of Vejbæk & Britze 1994
SALTPUTE XYZ	Salt pillows of Vejbæk & Britze 1994

In all files, X and Y are in meters. Total magnetic field and high passed field are in nanoteslas. Analytic signal is in nanoteslas per meter. Central meridian of UTM coordinates, 9 degrees East (UTM-zone 32, ED50 datum)

!!!To load these files, use the command: tar -xvb 1/dev/mt

The files were produced by a Windows NT system, but can be read by UNIX systems. The above information is also on the cassette as a readme file.

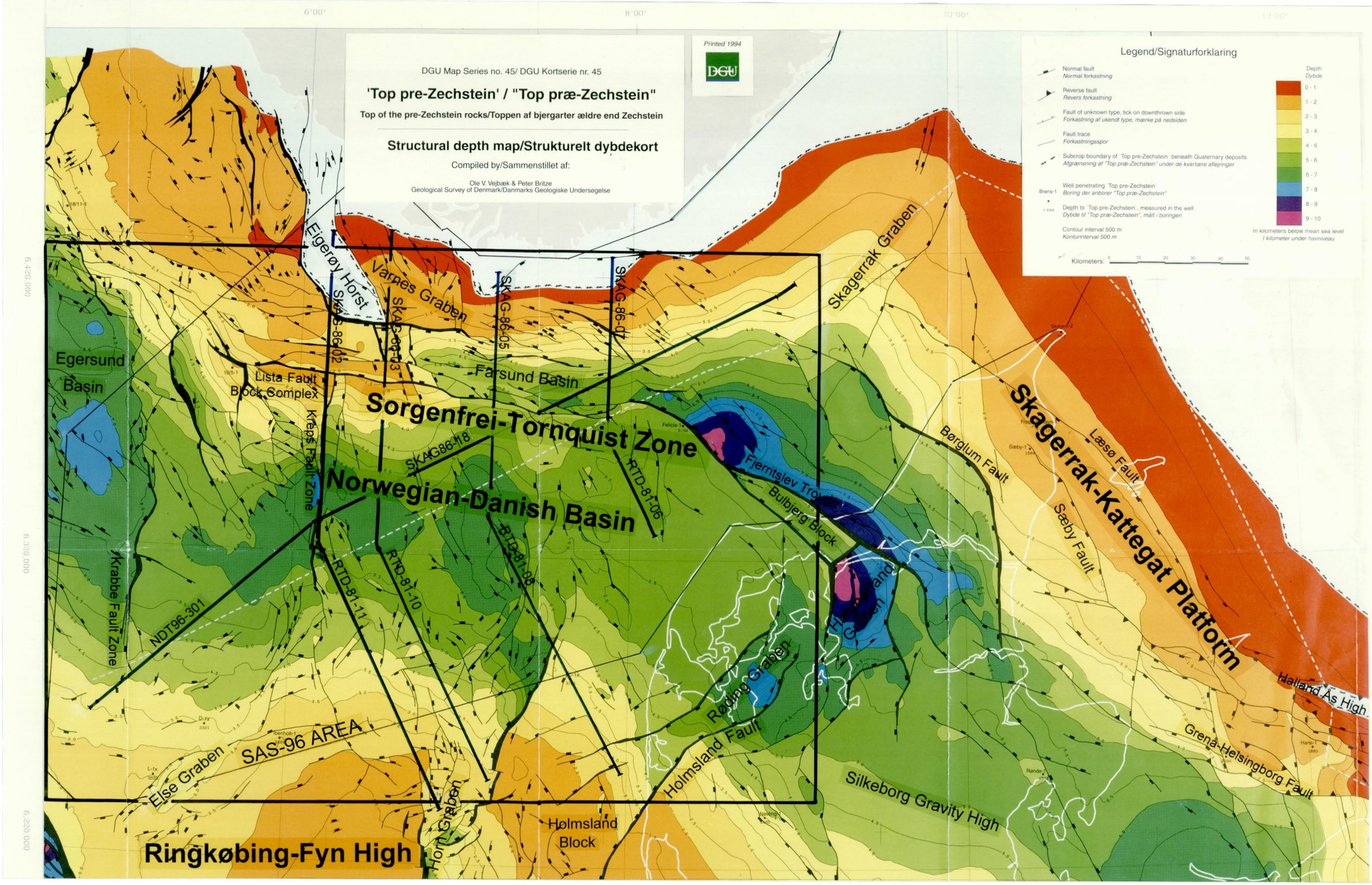

Fig. 2.1 Map of structural elements within the survey area. Reduced part of the Geological map of Denmark 1:750,000, Top pre-Zechstein, Structural depth map (Vejbæk & Britze 1994). Names of structural elements are added to the map. The thin black polygon shows the SAS-96 area which extends northwards to the outer Oslofjord. The bold black frame shows the location of the 1:250.000 maps (Maps 2-7, W1 and Figs. 4.3-4.6). The location of five interpretation profiles each consisting of two seismic lines are shown on the map SKAG-86-02 and RTD-81-11, SKAG-86-03 and RTD-81-10, SKAG-86-05 and RTD-81-08, SKAG-86-07 and RTD-81-06, NDT96-301 and SKAG86-18.

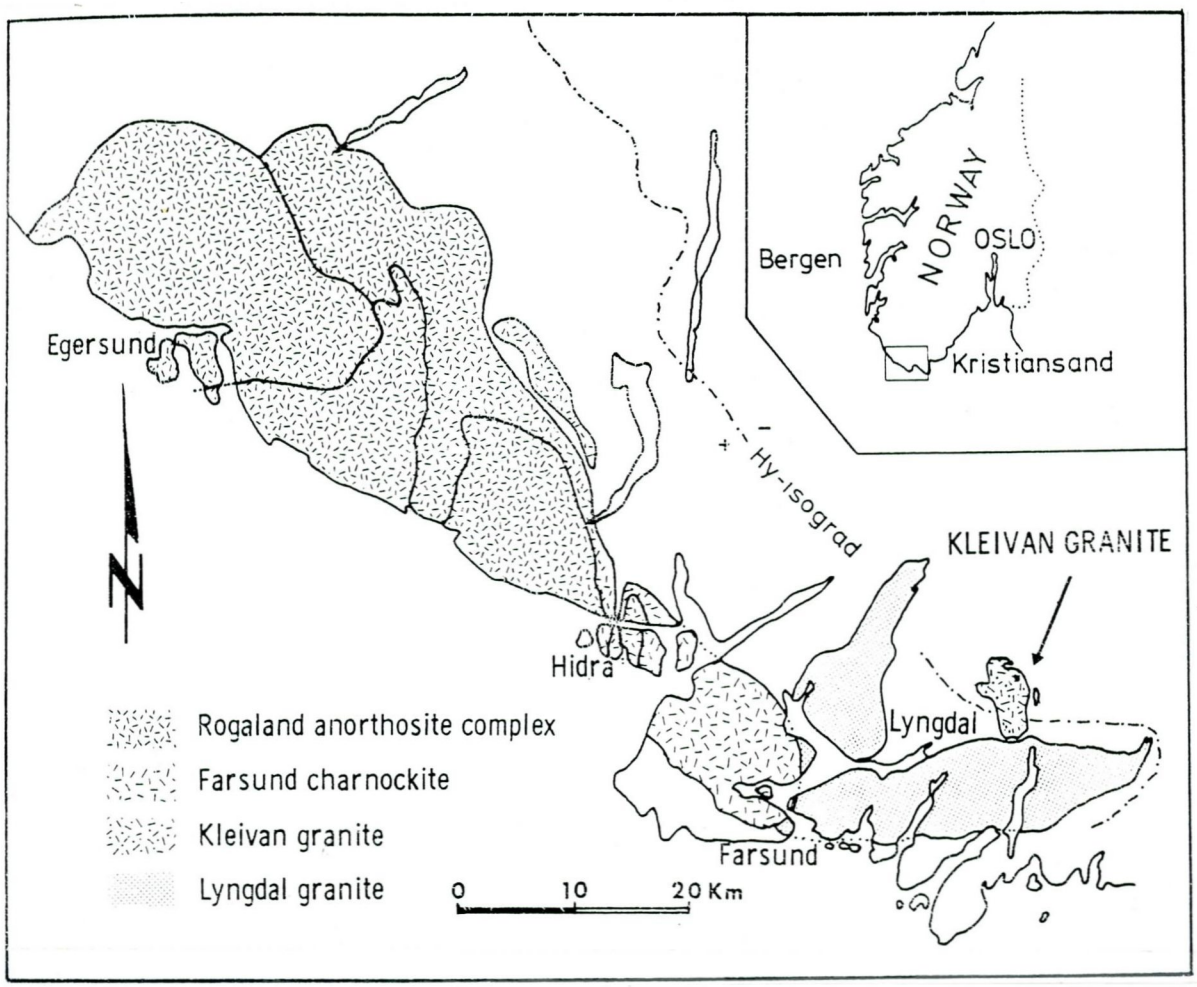

Fig. 2.2 Regional geological sketch map of the Rogaland Igneous Complex showing the spatial relationships between the Egersund Anorthosite Complex, the Farsund Charnokite and Lyngdal Granite (Falkum 1987). The E-W trend of the latter indicates that this Sveconorwegian trend may also prevail in the basement below the Farsund Basin. The E-W trending gravity and magnetic anomalies offshore Farsund-Kristiansand are more likely related to a southeastward continuation of the Rogaland Igneous Complex than to Permian igneous activity. The negative magnetic anomaly which has earlier been attributed to a Tertiary and/or Permian Skagerrak Volcano (Sharma 1970, Åm 1973) offshore Kristansand, is more likely caused by a reversed magnetised mafic body within this Sveconorwegian igneous complex (see Fig. 5.5).

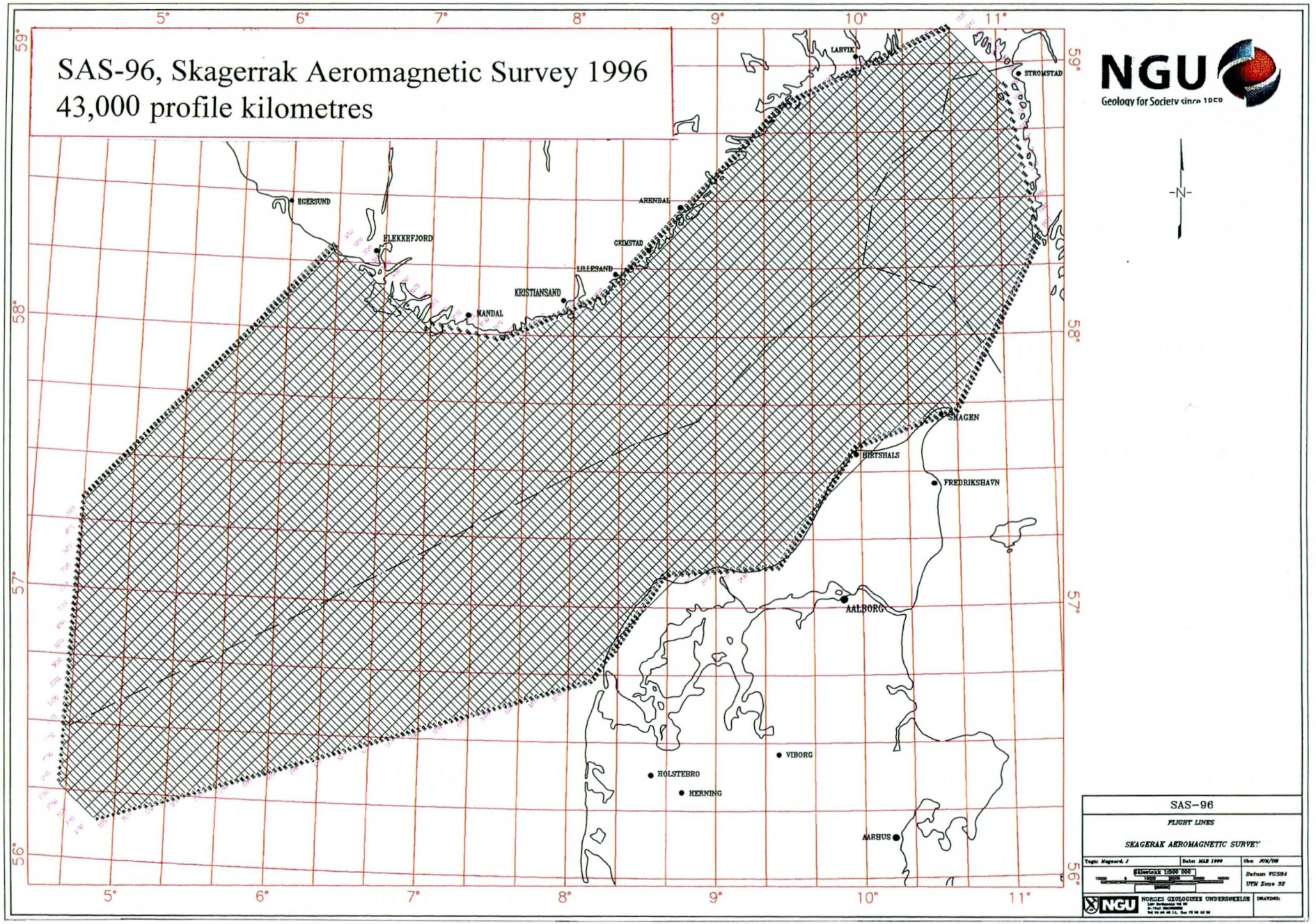

Fig. 3.1 Flight pattern diagram and map sheet layout of the SAS-96 aeromagnetic measurements. The survey was flown with a line spacing of 2 km and a tie-line separation of 5 km.

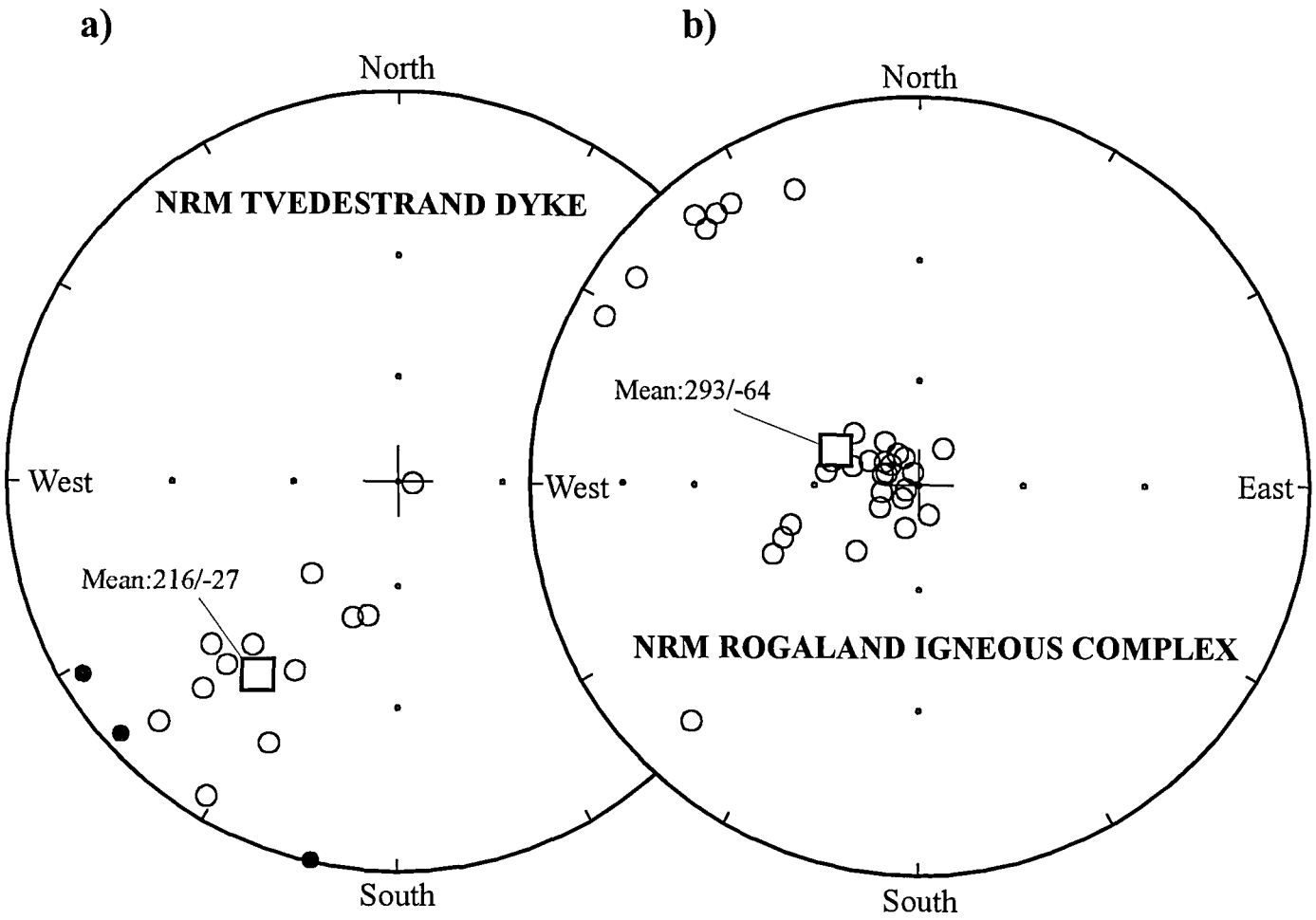

Fig. 3.2 Plot of natural remanent magnetisation (NRM) directions of a) Permian diabase from the Tvedestrand area (Torsvik in prep.) and b) Sveconorwegian norite from the Tellnes area, Rogaland Igenous Complex (McEnroe *et al.* 1996). Filled circles show positive inclination and open circles negative inclination.

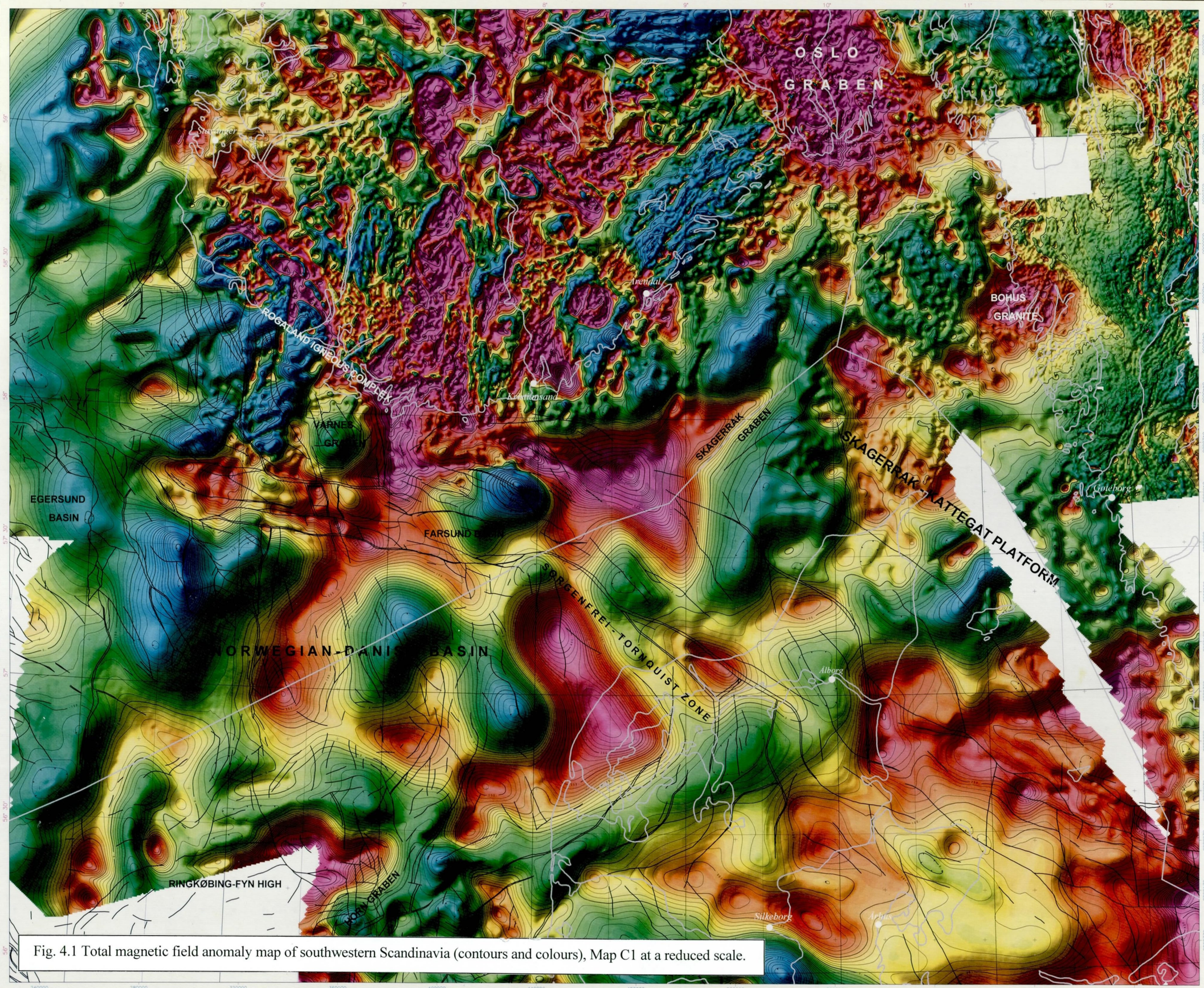

Fig. 4.1 Total magnetic field anomaly map of southwestern Scandinavia (contours and colours), Map C1 at a reduced scale.

OSLO GRABEN

BOHUS GRANITE

ROMMELAND IGNEOUS COMPLEX

VARNES GRABEN

EGERSUND BASIN

FARSUND BASIN

SKAGERRAK GRABEN

SKAGERRAK - KATTEGAT PLATFORM

SORGENFREI - TORNQUIST ZONE

NORWEGIAN - DANISH BASIN

HORN GRABEN

Stavanger

Arendal

Kristiansand

Göteborg

Ålborg

Silkeborg

Århus

NGU
Norges geologiske undersøkelse
Geological Survey of Norway

GEUS · HYDRO · Mobil · PHILLIPS 66 · STATOIL

39 29 25 21 18 15 13 10 8 6 4 2 0 -2 -4 -6 -8 -10 -12 -15 -19 -23 -29

Bouguer Gravity Field
(milli-Gal)

Shaded relief effect

Scale 1:500000
10000 0 10000 20000 30000
(metres)

GEODETIC DATUM: ED50
TRANSVERSE MERCATOR PROJECTION
Numbers in Blue: UTM coordinates, zone 32
Numbers in Magenta: Latitude and Longitude

CONFIDENTIAL
This map should not be circulated without the express permission of the Geological Survey of Norway

Fig. 4.2 Bouguer gravity anomaly map of southwestern Scandinavia (contours and colours), Map C2 at a reduced (contours and colours).

SKAGERRAK AEROMAGNETIC SURVEY 1996

Bouguer Gravity Anomaly Map
South-Western Scandinavia
Including top pre-Zechstein faults

Colour contour presentation
Shadowing applied with a virtual light source from the south-east

Geological Survey of Norway
Leiv Eirikssons vei 39
N-7040 Trondheim, Norway
in cooperation with:
Geological Survey of Denmark and Greenland
Norwegian Petroleum Directorate
Mobil Exploration, Norway Inc.
Norsk Hydro A/S
Phillips Petroleum Co., Norway
Statoil A/S

Data compilation: Odleiv Olesen
Data sources: NGU, GEUS, SK, NPD, Amarok, Mobil Statoil, N. Balling, I. Ramberg, S. Saxov, S. Smithson
Map production: Mark A. Smethurst
Map version: v. 1.0 12/5/97
Map number 97.022-C2

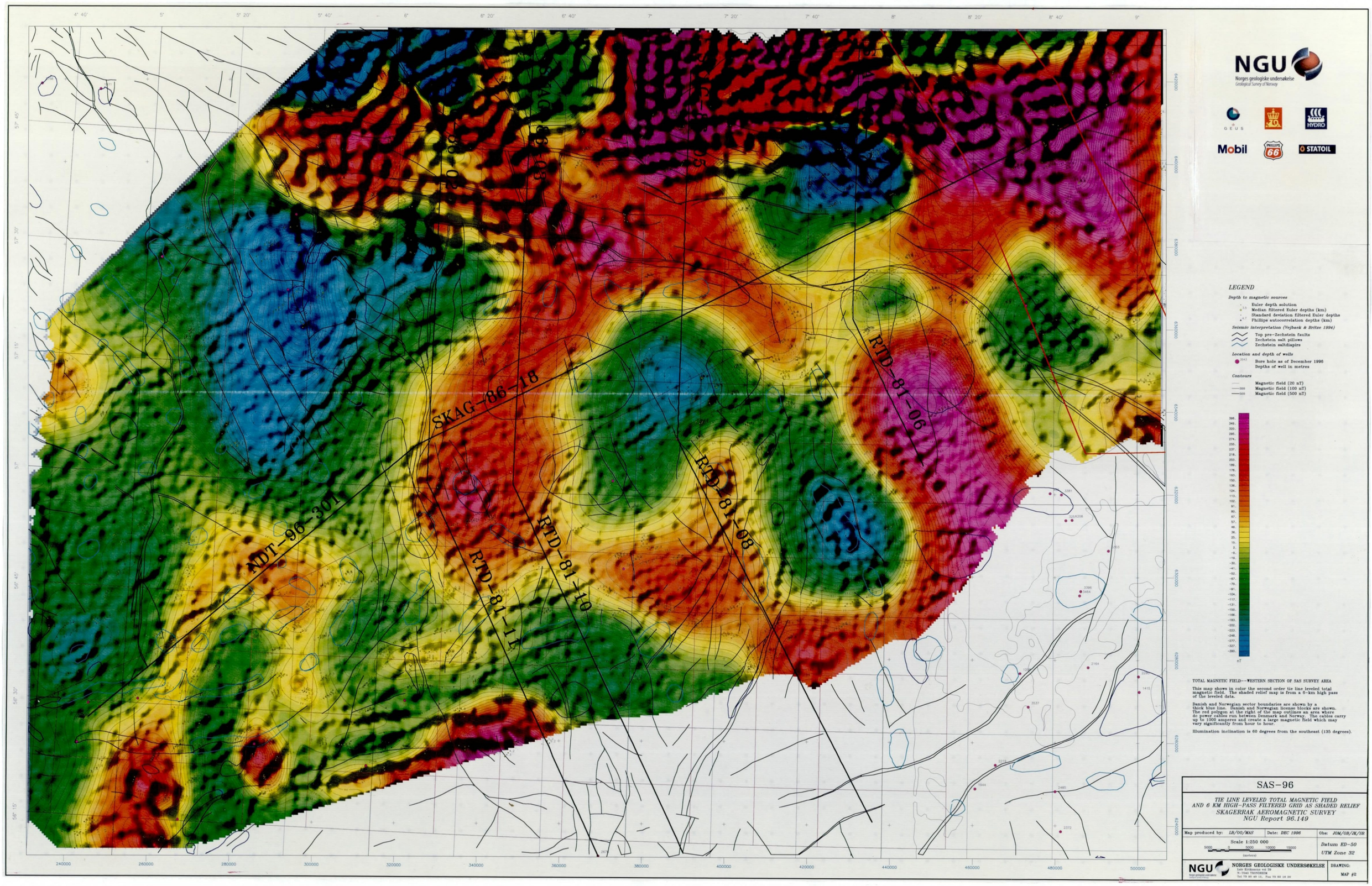

Fig. 4.3 Total magnetic field anomaly map, (contours and colours) and 6 km high-pass filtered grid as shaded relief, western SAS-96 area, Map 2 from SAS-96 Report Part I at a reduced scale.

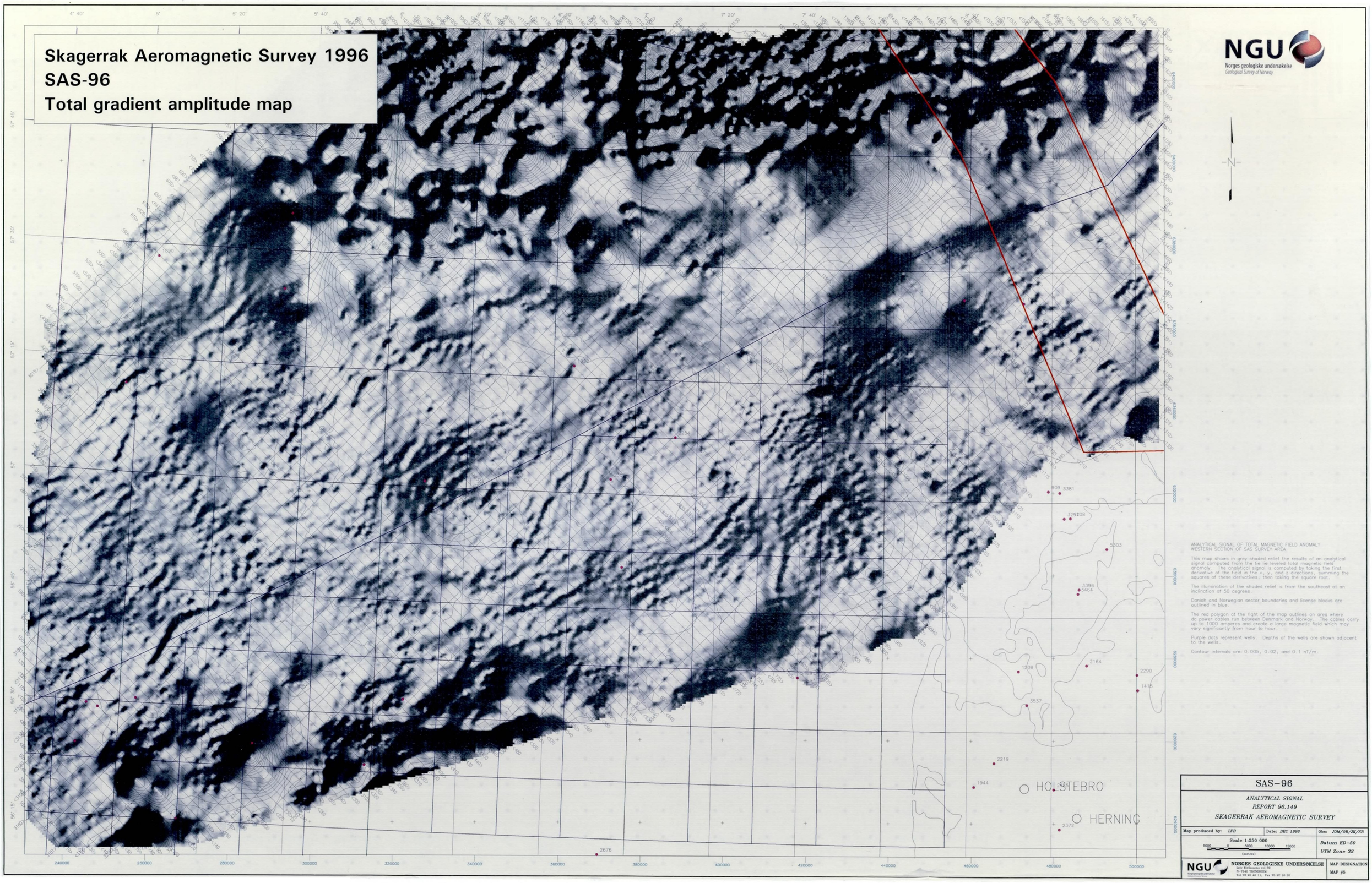

Fig. 4.4 Magnetic gradient amplitude map, Analytical signal, (contours and shaded relief, grey-tone), western area, Map 5 from SAS-96 Report Part I at a reduced scale.

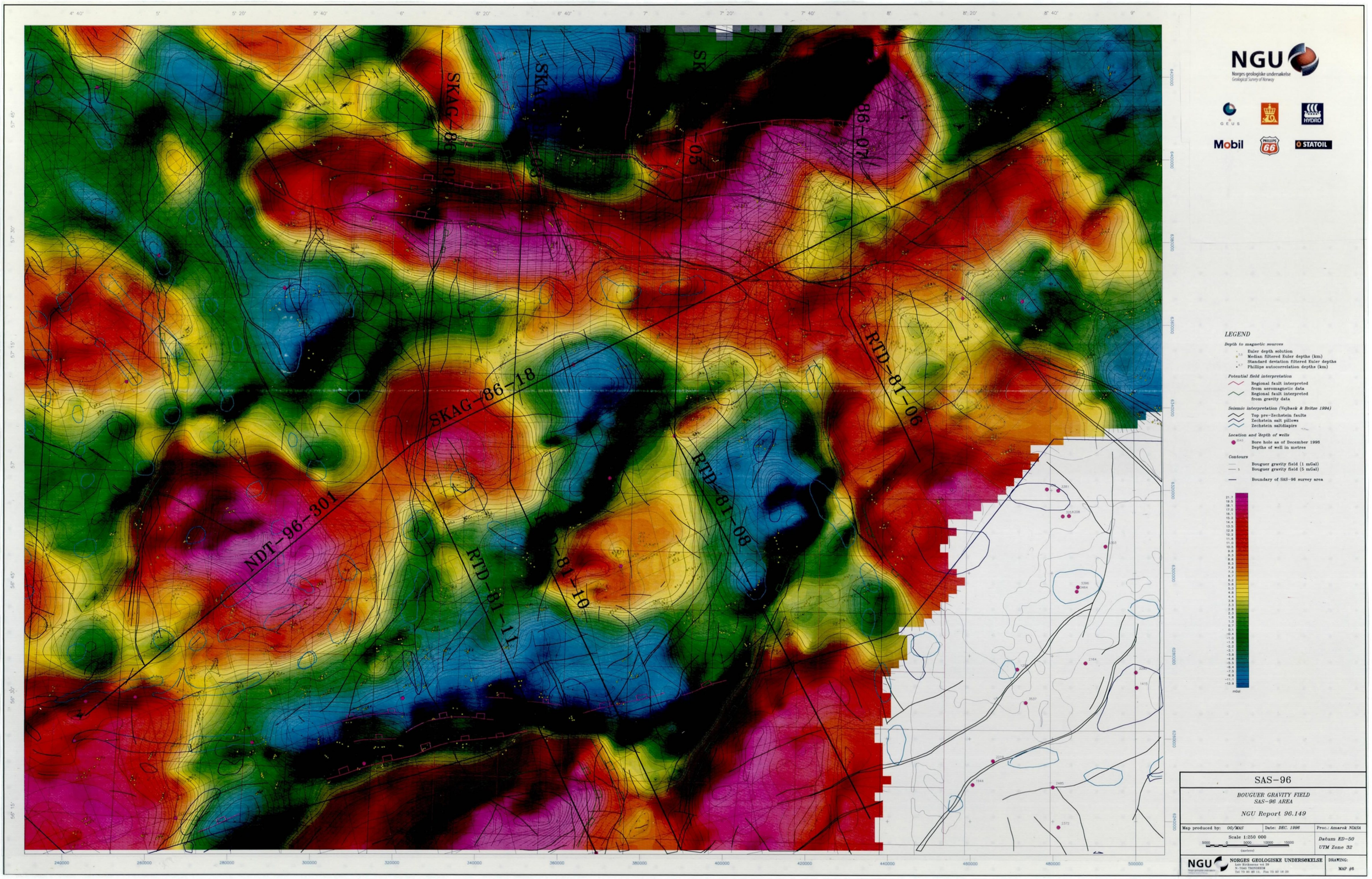

Fig. 4.5 Bouguer gravity map (contours, colours and shaded relief) with geophysical interpretations, western area, Map 6 from SAS-96 Report Part I at a reduced scale.

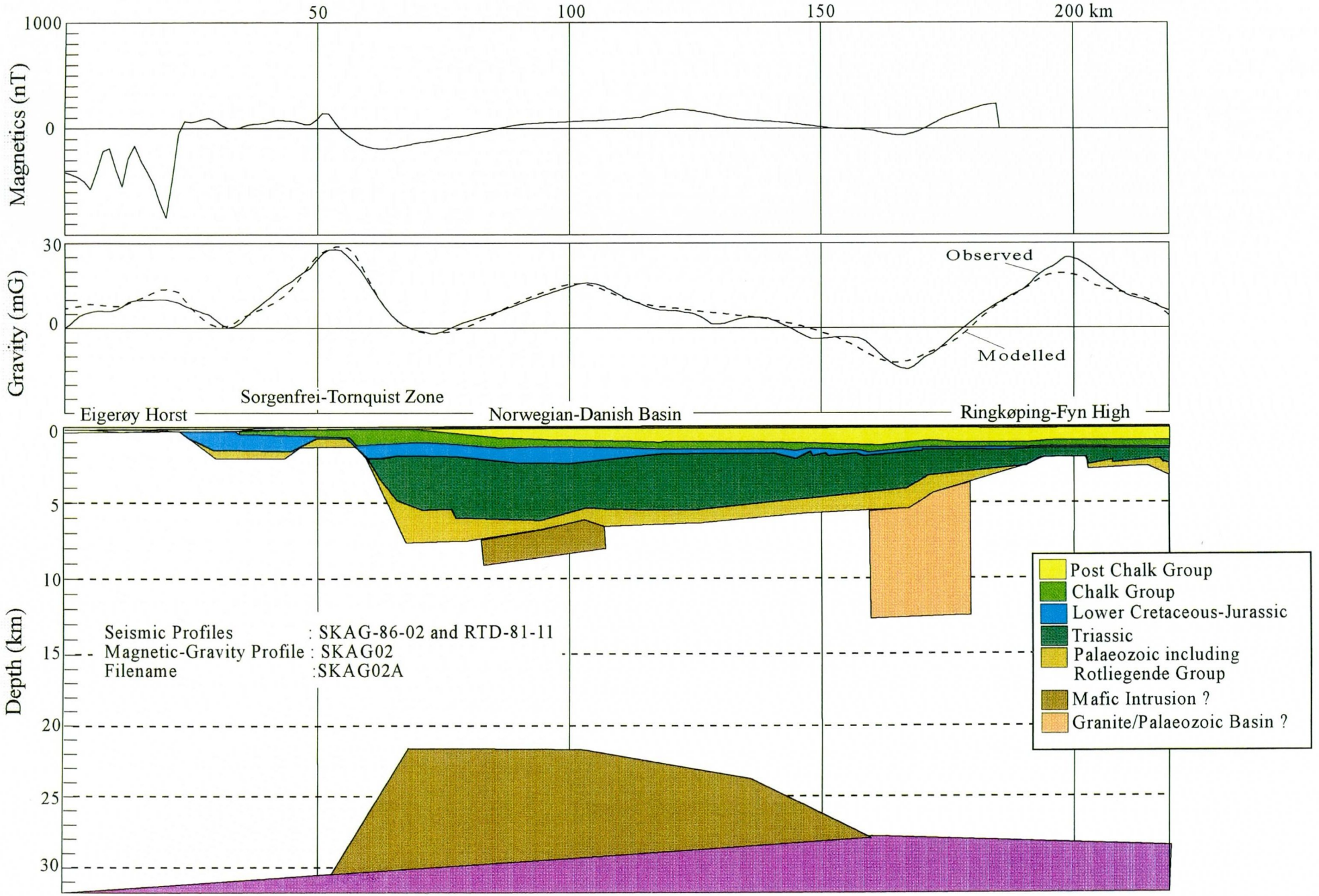

Fig. 5.1 Gravity interpretation along the seismic profile SKAG-86-02 and RTD-81-11 (Figs. 2, 6, 7 and 9, Maps 4, 5 and 9). Applied densities are shown in Table 3.4. Violet colour - mantle.

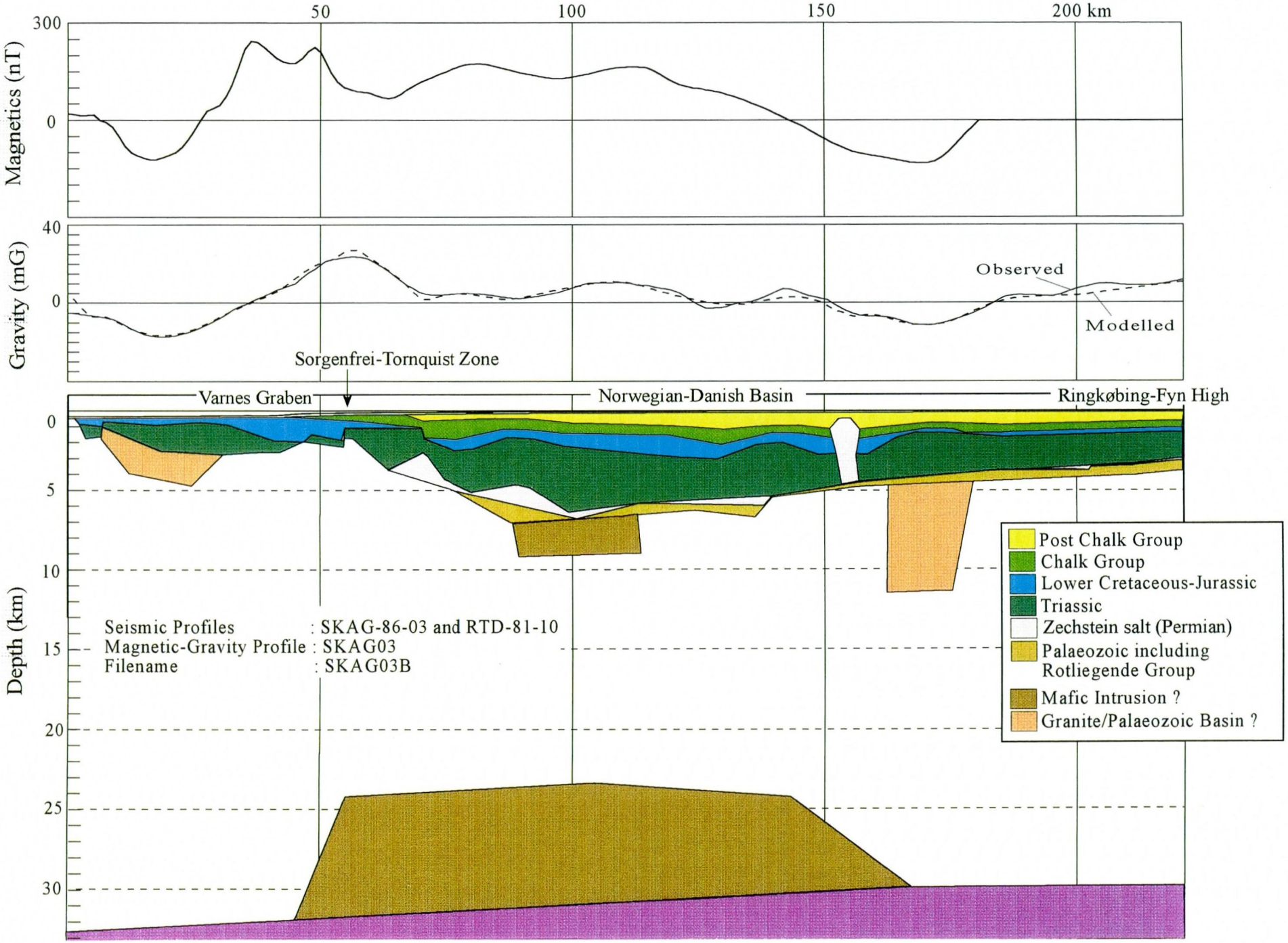

Fig. 5.2 Gravity interpretation along the seismic profile SKAG-86-03 and RTD-81-10 (Figs. 2, 6, 7 and 9, Maps 4, 5 and 9). Applied densities are shown in Table 3.4. Violet colour - mantle.

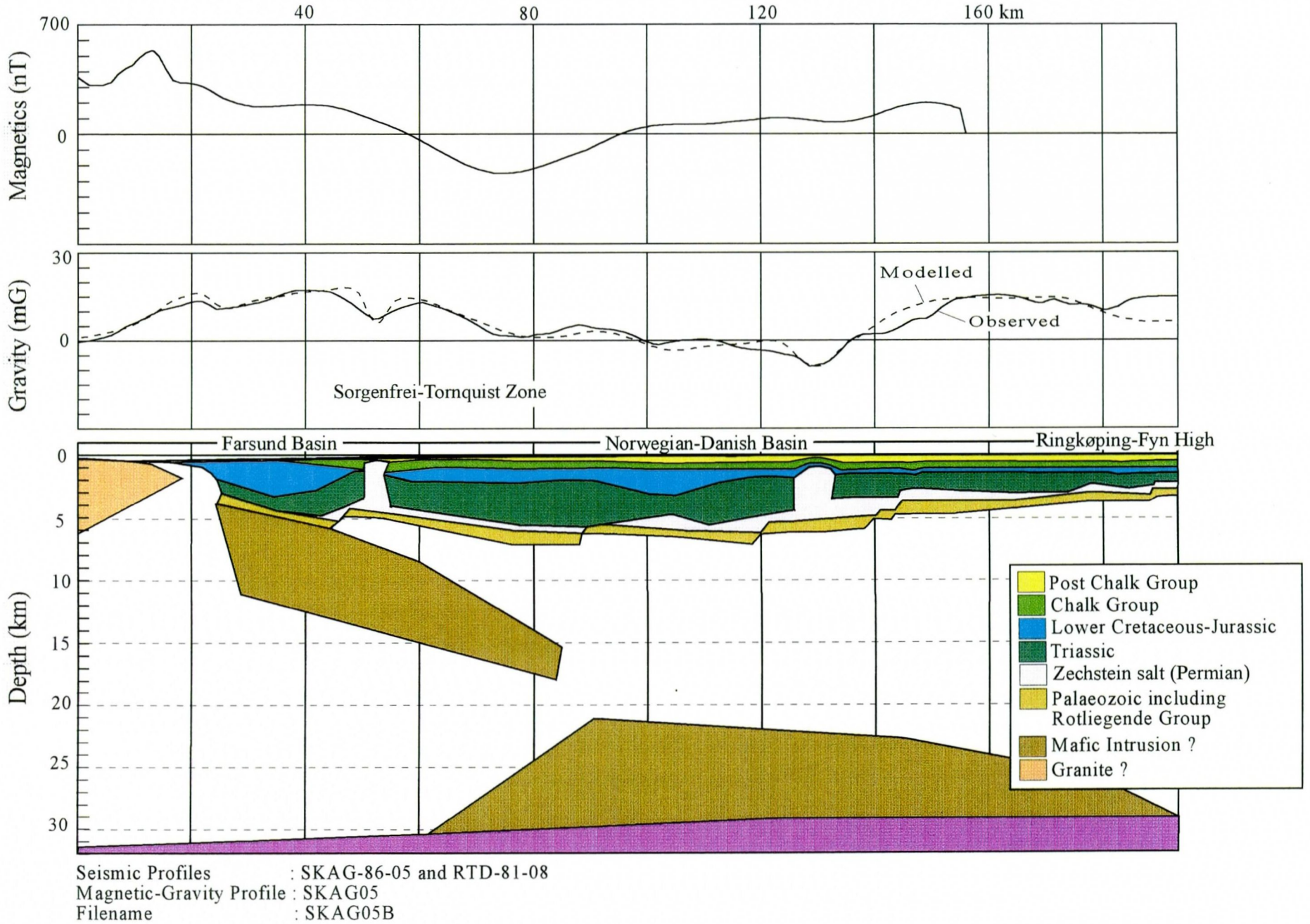

Fig. 5.3 Gravity interpretation along the seismic profile SKAG-86-05 and RTD-81-08 (Figs. 2, 6, 7 and 9, Maps 4, 5 and 9). Applied densities are shown in Table 3.4. Violet colour - mantle.

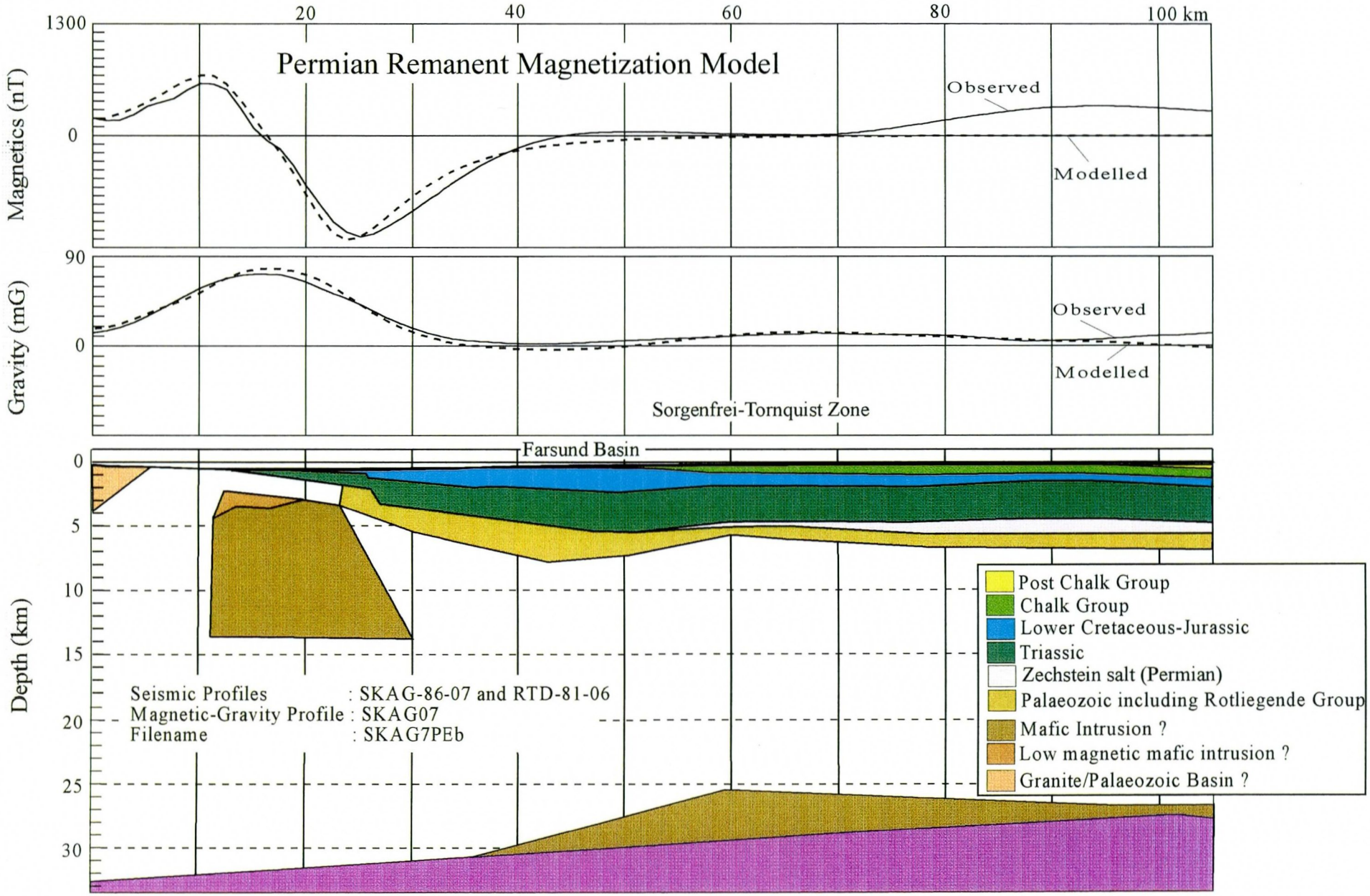

Fig. 5.4 Gravity and magnetic interpretation along the seismic profile SKAG-86-07 and RTD-81-06 (Figs. 2, 6, 7 and 9, Maps 4, 5 and 9). Applied densities and magnetic properties are shown in Tables 3.4 and 5.1, respectively. A Permian NRM direction is applied in the magnetic modelling. Violet colour - mantle.

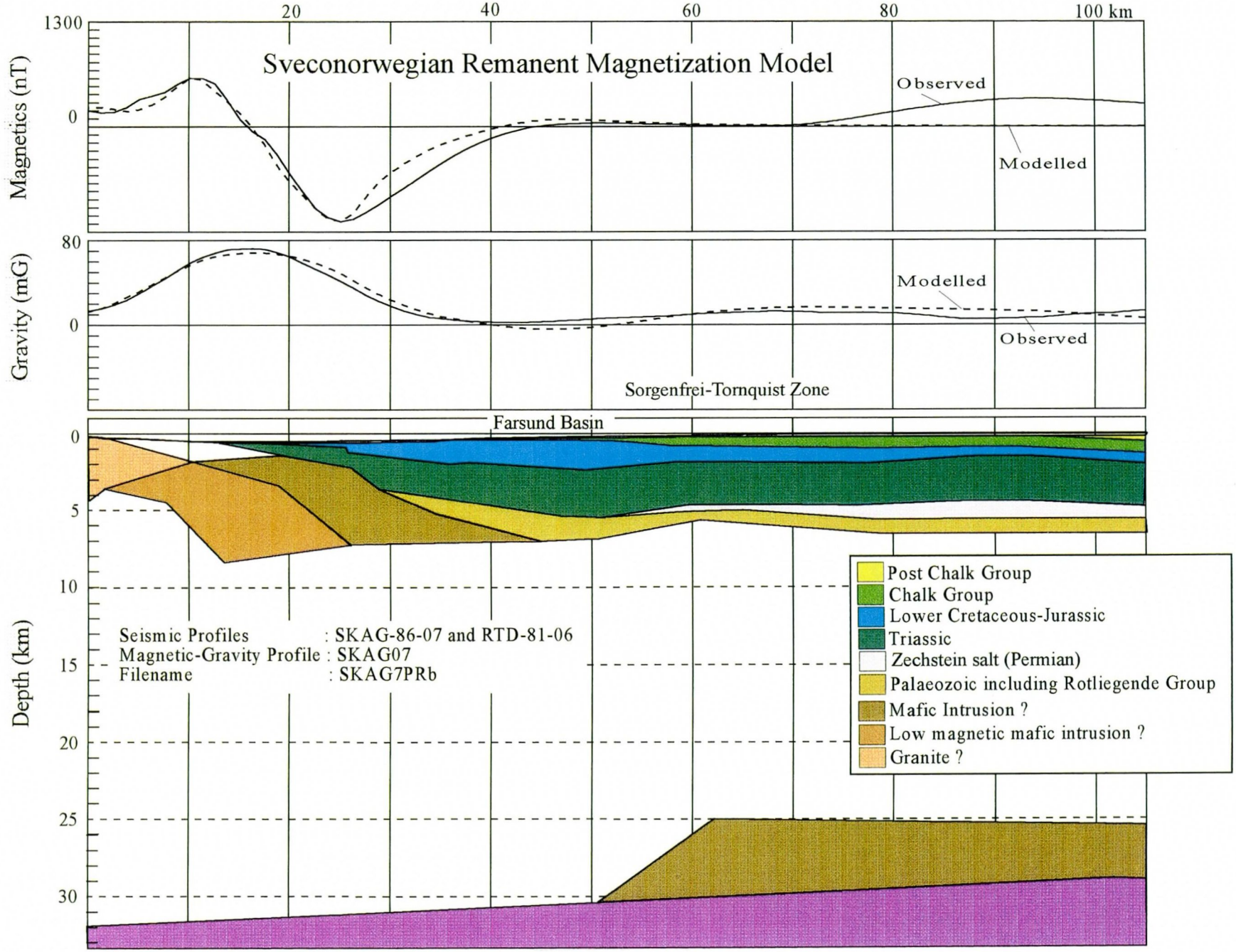

Fig. 5.5 Gravity and magnetic interpretation along the seismic profile SKAG-86-07 and RTD-81-06 (Figs. 2, 6, 7 and 9, Maps 4, 5 and 9). Applied densities and magnetic properties are shown in Table 3.4 and 5.1, respectively. A Sveconorwegian NRM direction is applied in the magnetic modelling. Violet colour - mantle.

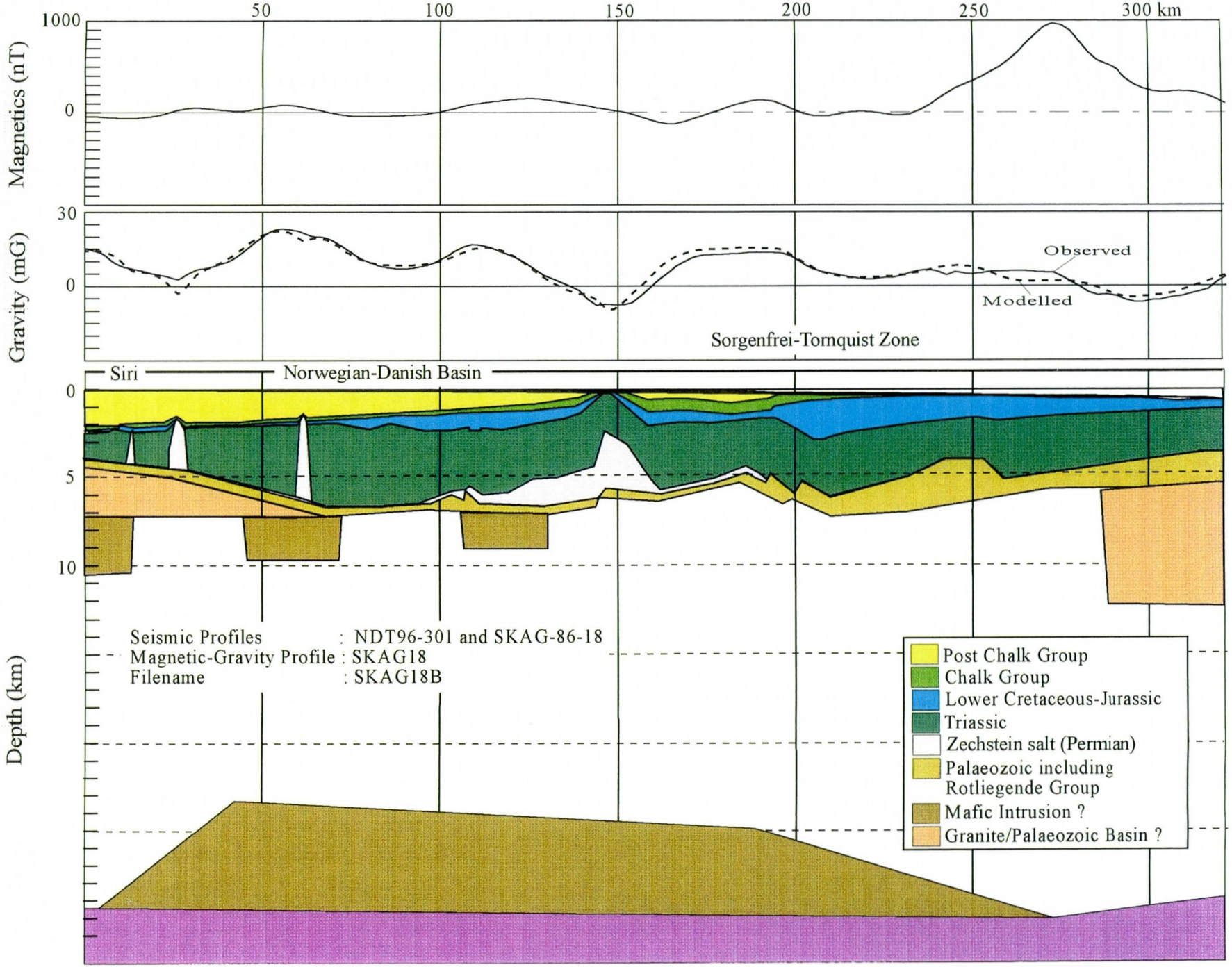

Fig. 5.6 Gravity interpretation along the seismic profile NDT96-301 and SKAG-86-18 (Figs. 2, 6, 7 and 9, Maps 4, 5 and 9). Applied densities are shown in Table 3.4. Violet colour - mantle.

Skagerrak Aeromagnetic Survey 1996
SAS-96
Geophysical interpretation map

NGU
Norges geologiske undersøkelse
Geological Survey of Norway

LEGEND

Depth to magnetic sources
- Euler depth solution
- Median filtered Euler depths (km)
- Standard deviation filtered Euler depths
- Phillips autocorrelation depths (km)

Potential field interpretation
- Regional fault interpreted from aeromagnetic data
- Regional fault interpreted from gravity data
- Sediment-related high-frequency aeromagnetic anomaly
- Boundary of reversed magnetised Egersund Anorthosite Province

Seismic interpretation (Vejbæk & Britze 1994)
- Top pre-Zechstein faults
- Zechstein salt pillows
- Zechstein saltdiapirs

Location and depth of wells
- Bore hole as of December 1996
- Depths of well in metres

Boundary of SAS-96 survey area

SAS-96

GEOPHYSICAL INTERPRETATION MAP
SAS-96 AREA

NGU Report 96.149

Map produced by: OO/MAS	Date: DEC. 1996	Proc.:
Scale 1:250 000 (meters)		*Datum ED-50* *UTM Zone 32*
NGU NORGES GEOLOGISKE UNDERSØKELSE		DRAWING: MAP #7

Fig. 5.7 Geophysical interpretation map, western area, Map 7 (SAS-96 Part I Report, Olesen *et al.* 1996) at a reduced scale.

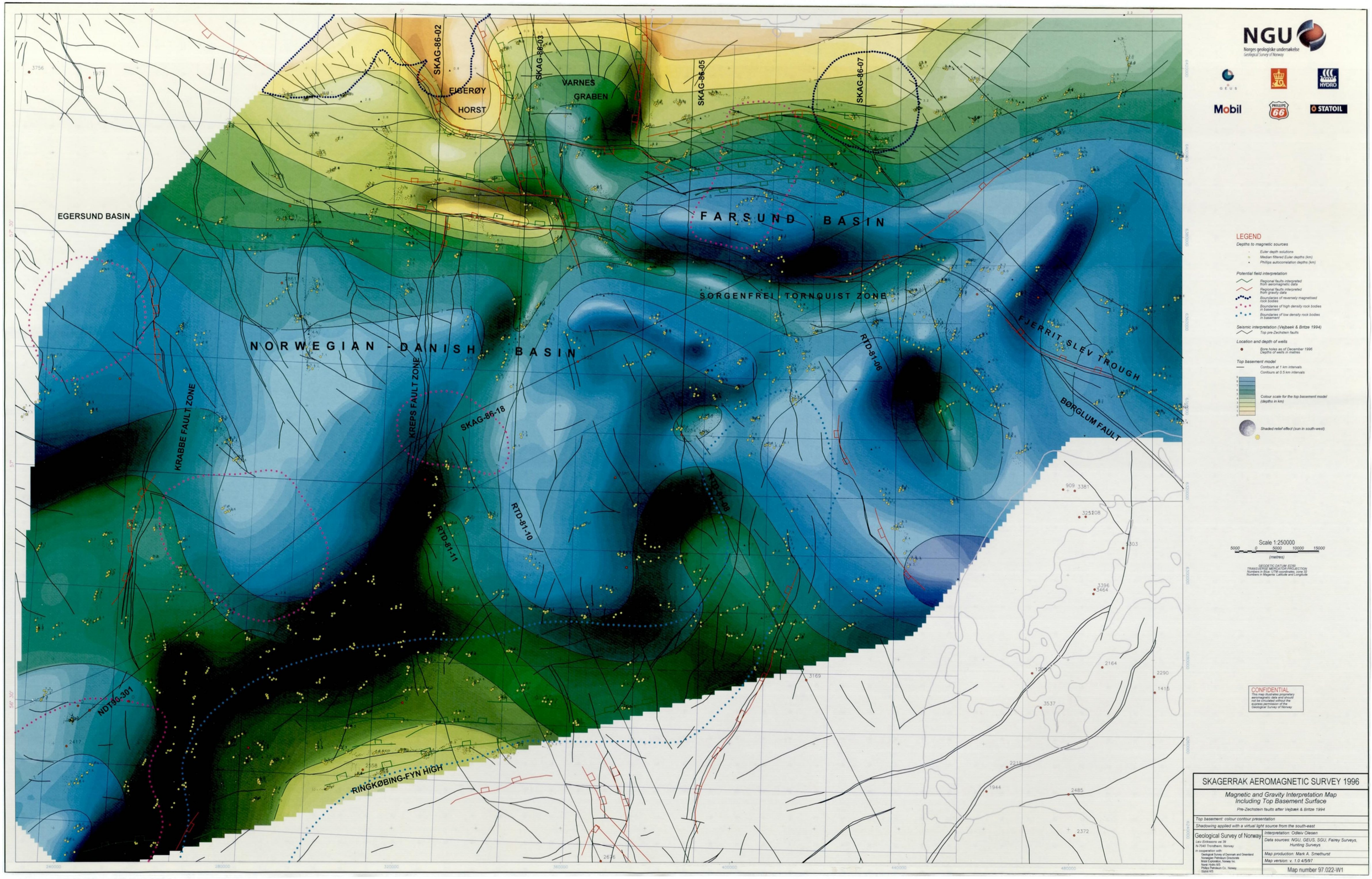

Fig. 5.8 Depth to magnetic basement interpretation map, western area, Map W1 at a reduced scale.

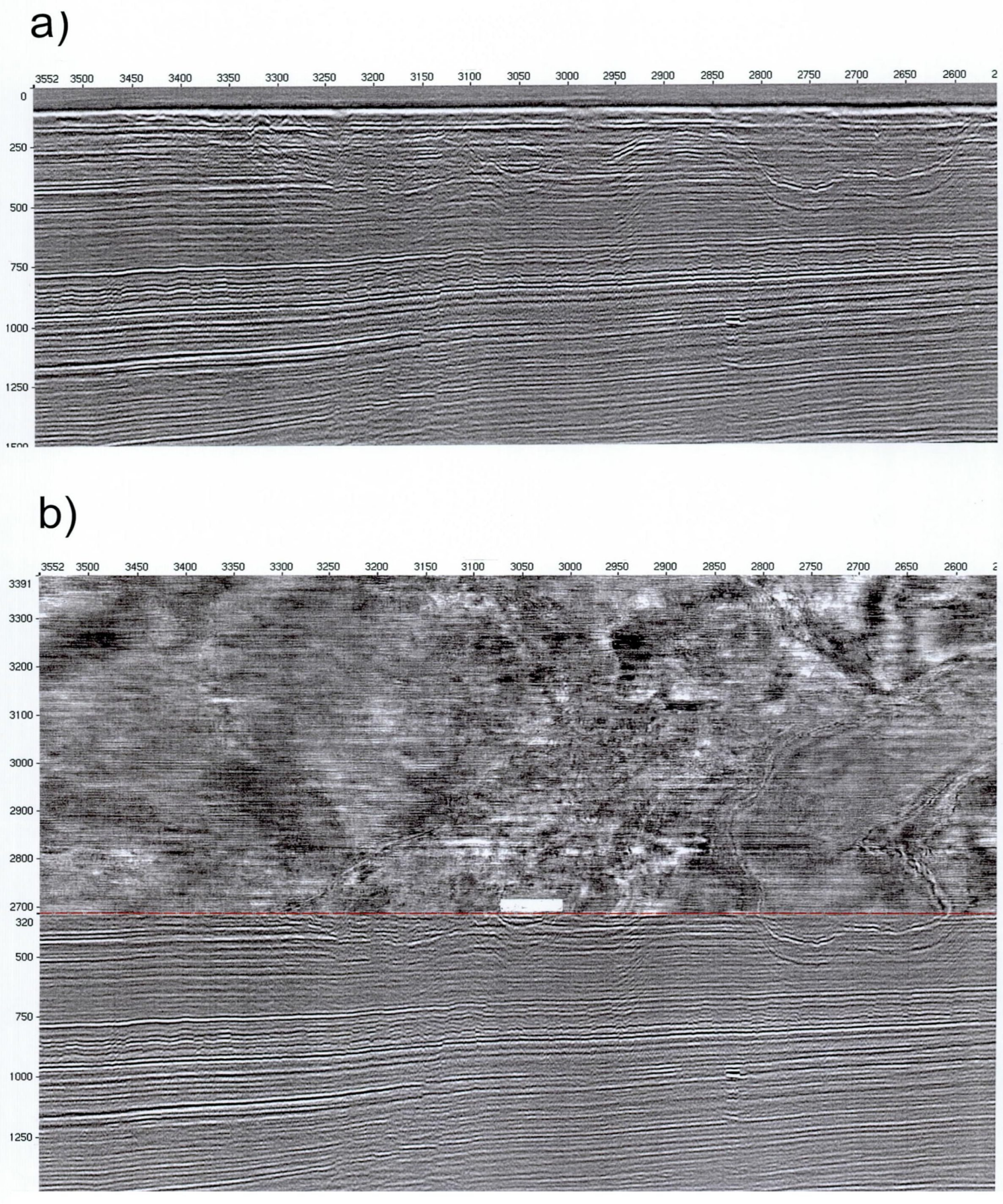

Fig. 5.9(a) Seismic section and (b) chair diagram from a 3D seismic cube in the Siri area showing Pleistocene sand channels coinciding with high-frequency aeromagnetic anomalies in the SAS-96 area (Figs. 4.3 & 4.4). Shot point distance 12.5 m.

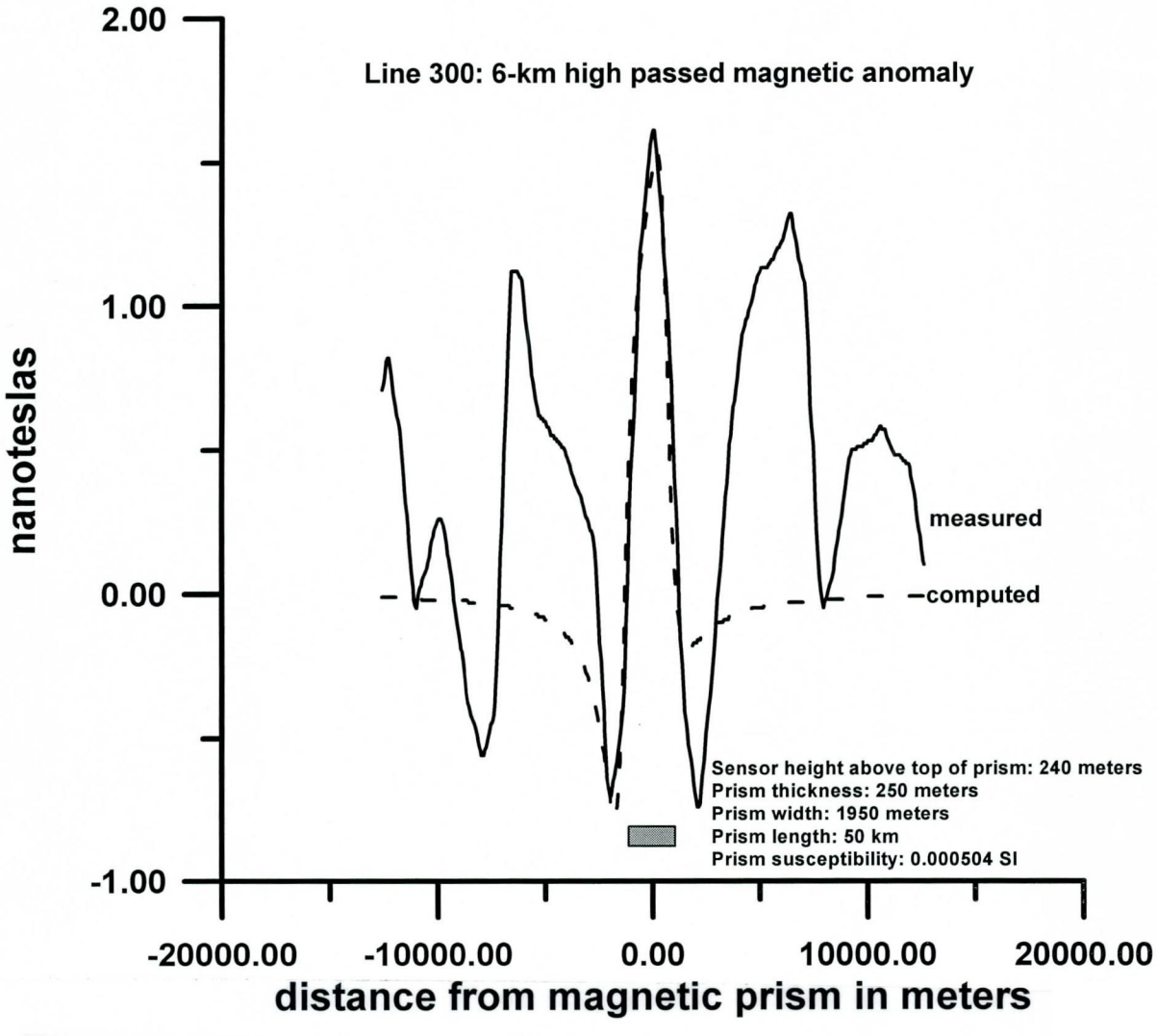

Fig. 5.10 Aeromagnetic modelling of a Pleistocene sand channel from the Siri area applying the algorithm by Bhattacharyya (1964).